Effect of dual-drug–releasing micelle-hydrogel composite on wound healing *in vivo* in full-thickness excision wound rat model

Monika Patel[1], Tadashi Nakaji-Hirabayashi[2, 3], Kazuaki Matsumura[1]*

[1] School of Materials Science, Japan Advanced Institute of Science and Technology, Ishikawa, 923-1292, Japan

[2] Graduate School of Science and Engineering ,University of Toyama, Toyama, 930-8555, Japan

[3]Graduate School of Innovative Life Science, University of Toyama, Toyama, 930-8555, Japan

* Corresponding author: [Kazuaki Matsumura e-mail: mkazuaki@jaist.ac.jp]

Abstract

Wound healing is a complex process involving an intricate cascade of body responses. A composite dressing that would effectively target different stages of wound healing and regeneration is urgently needed. In the current study, we tested the efficacy of a previously prepared micelle-hydrogel composite loaded with two drugs, in full-thickness excision wound model in rat. We found that the composite elicited almost no inflammation and effectively enhanced healing at all stages of the healing process. An initial burst of the first drug, amphotericin B, eliminated any preliminary infection. This burst was followed by a gradual release of curcumin as the healing and anti-inflammatory agent. Better healing was observed in rats treated with the drug-loaded composites than in blank and control groups. Wounds showed up to 80% closure in the treated group, with high collagen deposition. Re-epithelialization and granulation were also better in the treated group than in the non-treated control and blank groups. Histopathological examination revealed that drug-loaded composites improved cutaneous wound healing and regeneration. In conclusion, the micelle-hydrogel composite is an effective dressing and might have major applications in wound healing.

Keywords: Micelle-hydrogel composite, dermal wound healing, pH-sensitive release, dual-drug release, polypeptide hydrogel

INTRODUCTION

In the last few decades, development of new dressing material to aid wound healing has received great attention.[1-3] Although conventional (non-occlusive) wound dressings, which generate dry wound healing conditions, continue to constitute the largest type of dressing materials, the use of occlusive dressings,[4-6] hydrocolloid,[7, 8] and hydrogel dressings,[9-11] which offer hydrated wound healing conditions, is currently increasing. The next vital phase in the development of new dressing material is the development of material capable of delivering active molecules and/or drugs directly at the wound site. Indeed, dressings loaded with active factors and/or drugs are becoming increasingly popular because of the well-known fact that topical or exogenous application of active substances directly at the wound site improves healing.

Wound healing involves a series of complex and well-orchestrated events occurring after an injury or physical trauma to the skin,[12-13] that aims to completely restore the integrity of damaged tissue and reinstate it as a functional barrier.[14-16] However, in some extreme situations (i.e., trauma with large full-depth skin damage),[17] complete re-epithelialization takes a long time.[18] Therefore, extensive studies are focusing on wound dressing systems to promote better wound healing and to reduce scar formation.[19]

Wound dehydration perturbs the healing process,[20-22] compromising the optimal environment required by that process. Therefore, maintenance of the moisture of the wound is of prime importance for effective and fast wound healing. In such cases, hydrogels are a promising candidate material, with the ability to absorb wound exudates,[23-24] control wound dehydration, and allow oxygen access. Furthermore, in addition to the hydrated environment that hydrogels provide, they can serve an additional purpose, delivering bioactive substances directly to the wound in a sustained manner.

Curcumin[25-26] is the principle curcuminoid and active component of *Curcuma longa*. Chemically, it is diferuloylmethane, or 1,7-bis(4-hydroxy-3-methoxyphenyl)-1,6-heptadiene-3,5-dione, a naturally occurring low-molecular weight polyphenolic phytoconstituent. Curcumin, in a form of turmeric (powder of dried rhizome of *Curcuma longa*), has been widely and predominantly used in Asian countries, especially India[27] and China, as a dyeing material,[28] flavoring agent,[29] and in many forms of customary medical practices to treat a range of inflammatory and chronic ailments. Various studies involving curcumin present evidence in support of its numerous pharmacological benefits, such as anti-oxidant,[30, 31] anti-inflammatory,[32, 33] anti-bacterial,[34] anti-viral,[35] anti-tumor,[36] and hyperlipidemic activities. It has been reported that administration of curcumin, both topically and orally, results in rapid wound healing. Yet, the therapeutic efficacy of curcumin is restricted because of its poor solubility in aqueous media, reduced oral bioavailability, and high first-pass metabolism. Another disadvantage of curcumin is the means of application. Curcumin is a polyphenol, which can result in toxicity if applied in a highly concentrated dose. Hence, a water-soluble formulation with a controlled release would be preferred for clinical application of curcumin.

We recently reported preparation of a new micelle-hydrogel composite.[37] The composite consists of polypeptide micelles cross-linked with genipin, both of which are biocompatible and frequently used for medical purposes. The micelle-hydrogel composite is composed of two oppositely charged polypeptide-based micelle systems, the positively charged poly(L-lysine)-*b*-poly(phenylalanine) (PLL-PPA), and negatively charged poly(glutamic acid)-*b*-poly(phenylalanine) (PGA-PPA). Because of the presence of amphiphilic polypeptide chains, these polypeptides easily self-assemble into micelles, rendering drug loading of the hydrophobic core effortless and facile. In a previous study, we showed that these micelle systems release drugs

under various conditions.[37] Because of the opposite charge of the micelles in the composite, the two micellar systems behave differently at varying pH values, hence enabling various drug release rates. This phenomenon makes it easy to tune the release rate of different drugs from these different micelle types in the composite, making it an ideal candidate for dual-drug release studies, especially for wound healing studies.

The aim of the current study was to evaluate the *in vivo* biocompatibility and efficacy of the micelle-hydrogel composite[37] as a wound dressing, serving as a reservoir for sustained delivery of curcumin (Figure 1). We evaluated the activity of the prepared composite in wound healing *in vivo*, in a full-thickness excision wound model in rat. Biomechanical tests, biochemical analysis, and histopathological examinations were also conducted to investigate the therapeutic effects of curcumin-loaded micelle hydrogel composites in the model.

MATERIALS AND METHODS

Preparation of dual-drug–loaded micelle-hydrogel composites

The dual-drug–loaded micelle-hydrogel composites were generated by using poly(L-lysine-*b*-phenylalanine) and poly(glutamic acid-*b*-phenylalanine) (Scheme S1) polymers, as previously described[37] (Supporting Information). The polymers were synthesized using the common N-carboxyanhydride (NCA) method. NCA were prepared using protected amino acids (Scheme S2). The generated polymers (PLL-PPA and PGA-PPA) were dialyzed in solutions containing curcumin and amphotericin B (respectively) to form drug-loaded micelles and were then gelled using genipin (Scheme S3) to form a micelle-hydrogel composite.

Wound model

Wound generation. Adult (9-week-old, 290−310 g, $n = 25$ male Sprague−Dawley rats (Japan SLC, Inc. Shizuoka, Japan) were housed under a 12-h light/12-h dark cycle with *ad libitum* access to food and water. All animals were in quarantine for a week before the study. All manipulations were performed under aseptic conditions. NIH guidelines (or for non-U.S. residents similar national regulations) for the care and use of laboratory animals (NIH Publication #85-23 Rev. 1985) have been observed. Further, all animal procedures were performed following the protocol approved by the ethical committee in University of Toyama (Toyama, Japan). All rats were treated humanely throughout the experimental period. Transplantation experiments with dual-drug–loaded micelle-hydrogel composites and control samples were carried out under anesthesia with isoflurane gas (250–350 mL/min, isoflurane: 1.5–2.5%) using the UNIVENTOR 400 anesthesia unit (Univentor, Zejtun, Malta) and according to the guidelines of the Animal Welfare Committee of University of Toyama and Ministry of Education, Culture, Sports, Science and Technology

115 (MEXT). A standard full-thickness excision wound was created for the purpose of the study.
116 Briefly, on day 0, rats were anaesthetized, and the dorsum shaved and cleaned using saline-soaked
117 gauze, and then swabbed with 70% ethanol. A single full-thickness wound (20 mm × 20 mm) was
118 created in the left dorsal flank skin of each rat to the depth of the loose subcutaneous tissues, and
119 was left open (Figure 2).
120 ***Treatments.*** Animals were divided into four groups (6 rats per group). The wounds were topically
121 treated with a single application of blank hydrogels (without drugs); low-concentration hydrogels
122 (LC; hydrogels loaded with low concentration, 0.5 mg, of curcumin); or high-concentration
123 hydrogels (HC; hydrogels loaded with high concentration, 1.5 mg, of curcumin). Both LC and HC
124 groups were loaded with low concentration (50 μg) of amphotericin B to demonstrate dual-drug
125 release as well as prevent any infections of the wound. The wounds in the final group of animals
126 (the control group) were dressed using medical gauze. A piece of Tegaderm (3M, Maplewood,
127 MN, USA) was placed on top of all wounds to prevent the rats from removing the treatment
128 material. Upon experimental wounding, animals were housed in individual cages, and maintained at
129 an ambient temperature (23°C), with 12-h light/12-h dark cycles, with *ad libitum* access to food and
130 water.
131 For biochemical studies, histopathological examinations, and antioxidant enzyme analysis,
132 animals (3 rats per group) were sacrificed under anesthesia on days 4 and 8 after surgery, because
133 the most pronounced changes in tissue occur during the first week after wounding. Wound collagen
134 content, granulation tissue formation, wound maturity, and superoxide dismutase (SOD) and
135 catalase activity were investigated in detail as described below.

Histopathological examination

Adjacent skin fragments were removed together with the wound area to evaluate any histopathological alterations. The collected specimens were fixed in 10% buffered formalin, processed, embedded in paraffin, and then sectioned perpendicular to the wound surface into thin sections following standard protocols. Tissue sections were stained with hematoxylin and eosin, and analyzed using light microscopy (Biozero Keyence BZ 8000, Osaka, Japan). Tissue sections were also stained with rabbit anti-Iba1 IgG antibodies (Wako Pure Chemical Corp., Osaka, Japan) and Alexa488-conjugated anti-rabbit IgG antibodies (ThermoFisher Scientific, Waltham, MA, USA) to visualize macrophages, and counter-stained with Hoechst 33258 (DOJINDO Laboratories, Kumamoto, Japan) following the manufacturers' instructions.

Wound healing and wound closure evaluation

Wounds were digitally photographed together with an identity plate and calibration bar immediately after wounding, and subsequently after dressing removal and cleansing with sterile saline on days 4 and 8 (following re-anaesthetization, as above). Wound closure was determined based on scaled digital images of each wound using Image J image analysis software. Wound closure was calculated by measuring the open wound area in each digital image, at each time point. Open wound area was calculated as % of the original area immediately after wounding on day 0, by using the following formula:

$$\%\ wound\ closure = \frac{[wound\ area\ on\ day\ 0 - wound\ area\ on\ day\ X]}{wound\ area\ on\ day\ 0} \times 100$$

Evaluation of granulation

Granulation tissue deposition in wounds was semi-quantitatively scored based on panoramic photomicrographs of hematoxylin- and eosin-stained sections in the center of each wound. The granulation was estimated as the depth of granulated tissue at the site of scarring, by two experienced observers who were unaware of the treatment group allocation.

Evaluation of craniocaudal wound contraction (re-epithelialization)

Percentage craniocaudal contraction (a histological measure of central wound contraction, in a craniocaudal dimension) was determined in hematoxylin- and eosin-stained sections in the center of the wound. Wound width was expressed as the percentage of the original central wound width based on wound images taken on day 0.

Evaluation of tissue inflammation

The extent of inflammation in the wound was evaluated in each group of animals by Hoechst 33258 and anti-Iba1 antibody staining of tissue samples.

Evaluation of enzyme activity

Tissue samples were washed with phosphate-buffered saline to remove adhering red blood cells. The samples were homogenized in ice-cold 0.1 M Tris-HCl, pH 7.4, containing 0.5% Triton X-100, and 5 mM β-mercaptoethanol. The obtained crude mixture was centrifuged for 25 min at 8000× *g* and 4°C, and the pellet containing cell debris was discarded. The supernatant contained the total tissue enzyme activity (cytosolic and mitochondrial). SOD activity was determined in the

supernatant using a method based on the reduction of nitro blue tetrazolium, with sample absorbance measured at 560 nm.[38] To determine the catalase activity, the supernatant was mixed with H_2O_2 and decrease in sample absorbance was recorded at 240 nm, as previously described.[39]

Evaluation of collagen content

Wounded tissue samples were frozen in liquid nitrogen and then freeze-dried by lyophilization. The lyophilized samples were then incubated overnight in 0.5 M acetic acid and homogenized. The homogenate was centrifuged at 12000g for 15min at 4°C and total collagen content determined using a total collagen assay kit (BVN K218-100; Biovision, CA,USA) as per manufacturer's recommendations.

Determination of the mechanical properties of hydrogels

Rheological properties of the gels were evaluated using a rheometer equipped with a 24.99-mm 2.069° cone (Rheosol G5000, UBM Co., Ltd., Kyoto, Japan). Hydrogels were prepared as for the wound-healing test. The dynamic storage (G′) and loss (G″) moduli of the hydrogels were determined by a frequency dispersion mode, between 0.01 and 10 Hz. All analyses were carried out at 37°C. For the analysis, mineral oil was placed around the sample circumference to prevent evaporation of water from the micelle-hydrogel composite.

Statistical analysis

All the variables were tested in independent experiments repeated three times. Values are reported as the mean ± standard error of the mean. Experimental data from different groups were compared

202 using one-way analysis of variance (ANOVA). A p-value < 0.05 in a two-tailed test was
203 considered statistically significant.

RESULTS

Rationale for the study

Our group has recently designed a polypeptide-based system that enabled a highly efficient control of the rate of drug release by varying a range of parameters, including pH.[37] Since wound healing is highly impacted by the pH of healthy tissue surrounding the wounded tissue, the observation had a valid implication for testing the developed system *in vivo*. Previous studies indicated that the pH of tissue in the vicinity of a wound is acidic during healing and that this acidic environment (approximately pH 4.5)[40] is automatically created around the wounded tissue by the body. This intrigued us as the developed composite system could be exploited in response to pH, thus potentially improving the healing environment. Further, to improve wound retraction and healing, infection at the early stages of healing would ideally be prevented. This prompted us to use a dual-drug release system to controllably release an anti-bacterial drug (amphotericin B) during early stages of healing, followed by a slow release of the healing drug (curcumin). Indeed, an *in vitro* assay (Figure 3) indicated a controlled and desired release profile of these drugs at pH 4.5, which strengthened the hypothesis that the polypeptide-based system could be used as a superior wound healing system.

Evaluation of the novel micelle-hydrogel composite *in vivo*

Macroscopic observations. The bio-efficacy of the newly formulated micelle-hydrogel composite as a wound dressing was evaluated *in vivo* in a subcutaneous implantation study in the rat model. Dorsal wounds were generated and dressed with hydrogel or gauze, as required, covered by Tegaderm, and various wound parameters were monitored over 8 d (Figure 2).

226 Wound healing progression in the control, blank, LC, and HC groups is shown in Figure 4.
227 Wounds treated with LC and HC micelle-hydrogel composites exhibited noticeable dryness and
228 no indication of pathological fluid oozing out. In addition, no signs of inflammation or infection
229 were apparent in these groups compared with the control and blank groups. Wound closure was
230 analyzed in each group as a percentage of the reduction in wounded area on days 4 and 8 [Figure
231 5(a)]. Animals treated with micelles containing high concentration of curcumin showed more
232 substantial wound closure (53.04 ± 4.26% on day 4; 87.32 ± 3.11% on day 8) than those treated
233 with gels loaded with low concentration of curcumin (22.23 ± 3.86% on day 4; 73.39 ± 4.03% on
234 day 8), blank (15.12 ± 2.92% on day 4; 32.67 ± 3.81% on day 8), or in the control groups
235 (7.31 ± 3.64% on day 4; 18.73 ± 6.21% on day 8).
236 The residual wound area was determined in each group, by measuring the open wound area
237 on days 4 and 8 [Figure 5 (b)]. Wounds began to close on day 4 and residual wound sizes were
238 reduced in all rat groups by the end of day 8. A drastic reduction in the residual wound area was
239 observed after 8 d of treatment with HC gels. By contrast, the largest residual wound area was
240 noted in the control group, indicating slow wound healing. Decrease of the wounded area is an
241 important parameter in wound healing, indicative of reduced infection and inflammation. Overall,
242 on days 4 and 8, wound contraction in HC group was significantly greater than that in other groups.
243
244 ***Microscopic observations.*** To evaluate wound closure in more detail, the effect of the treatments
245 on the process of granulation[41] and re-epithelialization[42, 43] was studied. Thickness of granulation
246 tissue and extent of re-epithelization were evaluated in hematoxylin- and eosin-stained tissue
247 samples. As shown in Figure 6, the granulation was significantly enhanced in wounds after 8-d
248 treatment with HC gels. However, no significant improvement in the granulation was apparent in

the control samples, which exhibited minimum or almost no granulation. In the blank group, granulation was moderate, and better than that in the control but significantly lower than of the LC and HC treated groups.

Re-epithelialization was analyzed in all test groups on days 4 and 8. As shown in Figure 7, no pronounced epithelial regeneration was apparent in blank and control groups on day 4. Conversely, in the LC and HC groups, enhanced formation of the epithelial lining was apparent as early as 4 d after wounding. Re-epithelialization was improved in all samples by day 8. These results were consistent with the analysis of the residual wound area. As shown in Figure 8, wounds treated with HC exhibited a well-defined regenerated and differentiated epidermal layer on day 8, with a fairly higher cell number and a relatively thicker dermis than wounds in other samples. Wounds in the LC group also exhibited an enhanced re-epithelialization but the effect was not as pronounced as in the HC group. Samples from other groups showed an early, on-going epithelial layer formation with poor granulation and traces of edema.

Effect on tissue inflammation. Hematoxylin and eosin staining supported the notion of enhanced wound healing in groups treated with HC and LC gels. To better understand the effect of the implanted gels on tissue and contribution to wound healing, the inflammatory response at implantation site was evaluated.[44-46] Wound tissue sections from different groups after 4-d and 8-d treatment were stained with Hoechst 33258 and anti-Iba1 antibodies.

And shown in Figure 9, on day 4 after surgery, an extremely high inflammatory response was noted in the control group, with a massive accumulation of macrophages at the wound site (green dots marking the cytosol of macrophages stained with anti-Iba1 antibodies). The accumulation of macrophages in the control group was reduced on day 8 after wounding but

remained appreciably higher than that in other groups. The second highest inflammatory response on day 4 was evident in the blank group. The response visibly declined by day 8. By contrast, in the remaining two groups (LC and HC groups), no accumulation of macrophages was apparent on day 4, indicating enhanced wound healing, with the cell proliferation phase already started. That was also suggested by the large number of accumulated cells in LC and HC samples (blue dots in Figure 9, stained by Hoechst 33258). On day 4, clear granulation was apparent in HC samples, indicative of accumulation of non-inflammatory cells, which by day 8 turned into a well-defined regenerated epithelium. Similarly, no visible signs of enhanced inflammation were apparent on day 4 in LC samples, with a clear onset of re-epithelialization by day 8, supporting the notion that the hydrogels improved wound healing in the LC and HC treatment groups.

Effect on tissue enzyme activity, collagen content, and angiogenesis. In addition to histological analysis, other biochemical wound parameters were evaluated to assess the efficiency of wound healing. Previous studies indicated that wounding induces oxidative stress in the injured tissue, enhancing the expression of SOD-encoding gene.[47] SOD activity was determined in injured tissues, and a clear reduction in the net SOD activity was observed. As shown in Figure 10, SOD levels in the HC and LC groups were reduced on days 4 and 8 in comparison with those in blank and control groups, where an increment in the level of SOD activity on day 8 was apparent. A contrasting trend was observed for the activity of catalase, another antioxidant enzyme (Figure 11). Accordingly, catalase activity on day 4 in the control and blank groups was similar to or higher than that in the LC and HC groups, whereas it was significantly increased by day 8. By day 8, catalase activity in HC group was almost double that in the control group.

The net collagen content[48-51] of the wounded tissues on days 4 and 8 after the surgery was next examined (Figure 12). As shown, the total collagen deposition was highest in the HC group on days 4 and 8, strongly indicating enhanced wound healing in comparison with other samples.

Since angiogenesis is a crucial parameter of the wound healing process, tissue sections were stained with anti-CD31 antibodies to evaluate the effect of treatments on the formation of blood vessels. As shown in Figure 13, wounds in the LC and HC groups contained more CD31-positive cells than those in the blank and control groups.

Rheological properties of the hydrogels

Finally, rheological properties of the hydrogels were evaluated to better understand hydrogel behavior. As shown in Figure 14, a composite lacking the PGA-PPA micelles showed a very low storage modulus (G′), in the range of 10^2 Pa, and a low loss modulus (G″), in the order of 10^1 Pa, in comparison with the composite with both micelles present, where the storage and loss moduli were in the range of 10^4 and 10^3 Pa, respectively. This suggested the role and importance of PGA-PPA micelles in the maintenance of gel structure and strength. The values of storage and loss moduli of the hydrogel steadily decreased over 48 h (Figure 15). This supported the notion of controlled drug release from the hydrogels.

DISCUSSION

In the current study, we evaluated the effectiveness of a novel dual-drug–releasing micelle-hydrogel composite in wound healing *in vivo*, in the full-thickness excision wound rat model.

The process of wound healing follows a distinct timeline of physical events (phases), including post-trauma repair in the case of an injury. In intact skin, the epidermis (upper skin layer) and dermis (deep skin layer) act as a defensive barrier against the external environment. When the barrier is broken, i.e., when the skin is injured, a coordinated cascade of biochemical reactions is brought into motion to heal the damage. The sequence of events includes blood clotting, inflammation, cell proliferation, and maturation (remodeling).

In the initial moments following the injury, platelets in the blood begin to accumulate at the site of injury.[52] The platelets become activated and release chemical cues to promote clotting. The resultant clot facilitates the closing of the opening in the blood vessel, preventing further bleeding. Inflammation is an important phase of wound healing.[53, 54] Cells that had been damaged or are dead as a result of the injury are cleared out. Inflammation also facilitates the removal of bacteria and other infectious pathogens. Proliferation marks the growth of new tissue at the injury site.[55, 56] The beginning of this phase accompanies the start of granulation, with new cells migrating to the site of injury and proliferating. Angiogenesis, connective tissue deposition, re-epithelialization, and wound contraction are the key events of the proliferation phase. Finally, tissue repair is completed in the maturation (remodeling) phase.[57] Then, the connective tissue is rearranged along tension lines, and cells that have served their purpose are strategically removed by programmed cell death (apoptosis).

To determine the effect of the micelle-hydrogel composite on different stages of wound healing, we performed various analyses, and reported strikingly positive results. The specific

composite was used because of its ability to release drugs in response to the need of the environment in the vicinity of the wound. At acidic pH (ca. 4.5), PGA chains in the PGA-PPA micelles become relatively un-charged and acquire a helical conformation, which strains the core of the micelle and results in faster release of the drug. This is required for the initial prevention of infection at the site of wounding.[37] On the other hand; PLL-PPA micelles in the composite exist in charged random-coil state. The micellar organization and drug release remain stable, releasing the drug slowly over a period of time, aiding wound healing (Figure S1).

We observed that in the LC- and HC-treated groups, wound size decreased with time in the absence of oozing or visible signs of infection. This supported the notion that the micelle-hydrogel composite accelerated wound healing. The blank and LC treatment groups showed an intermediate response between that of the control and HC groups. Granulation in the LC group was improved because of the regular supply of curcumin to the tissue by the implanted gels. Quantitative analysis of wound closure revealed a significant improvement in the LC and HC groups in comparison with the blank and control groups. The implanted micelle hydrogel composites prevented drying out of the wounds.

Several previous studies demonstrated the consequences of the innate immune response of resident cells and incoming inflammatory cells (such as monocytes and granulocytes) during skin wound repair.[58] These cells fight the invading microbes, contribute to scavenging of dead and decaying cells, and also (crucially) support the repair process by releasing a spectrum of growth factors. However, because of the release of pro-inflammatory and cytotoxic mediators, uncontrolled activity of macrophages may become detrimental to tissue repair. Indeed, imbalanced inflammation characterized by increased numbers of macrophages is a hallmark of attenuated repair response in human diseases, including diabetes mellitus,[59] vascular disease, and aging. Data

presented in the current study (Figure 6) indicated that the initial migration of cells was faster in the HC and LC groups than in the blank and control groups. This might be a consequence of the constant release of curcumin in the HC and LC groups, in agreement with published observations that curcumin considerably improves granulation in non-ischemic wounds.[60]

A series of important events takes place at the edge of the wound, accompanying granulation. Epidermal cells in the direct vicinity of the edge of the wound begin to thicken within the first 24–48 h post injury.[61] Basal cells at the edge start to flatten towards the wound, eventually covering the wound. The newly formed epithelium, however, is thinner than the normal (uninjured) epithelium. In large and open wounds, epithelialization proceeds over the bed of granulized tissue, involving the activity of proteolytic enzymes. The re-epithelialization process is evident in Figure 8, with a steady migration of cells towards wound closure (marked by a dotted line), proceeding over the course of few days. In typical wounded tissues, inflammation onsets and subsides by 2–3 d of wound creation, however, the exact time line depends on the type and location of the wound.[58, 62]

As the wound progresses through the inflammation phase, cell debris and necrotic tissues are cleared off, creating room for proliferation. Early onset of inflammation is essentially a sign of improved wound healing, indicating that the wound is rapidly going through the proliferation phase, in which fibroblasts migrate to the wound bed. Fibrin strands that facilitate fibroblast migration to the wound site are deposited in the inflammatory phase. As shown in Figure 9 wounds in the HC and LC groups progressed through the inflammatory phase by day 4, in contrast with the blank and control group, where the wounds contained very high numbers of macrophages at that time point (marking the inflammatory phase). The early onset and completion of inflammatory phase in the HC and LC groups may be attributed to curcumin, a strong anti-inflammatory drug.[63]

Analysis of the biochemical aspects of wound healing, including SOD and catalase activities, and the amount of collagen in wounded tissue, yielded interesting results. Wounding is a stressful event for any organism, not only causing discomfort and pain, but also initiating a cascade of events at the wound site. Oxidative stress is one of such of events, and is marked by the presence of superoxide radicals at the site of injury. As the radical concentration increases, so does the expression of SOD, a radical-scavenging enzyme.[64] Considering the antioxidant activity of curcumin, a model drug in the current study, we anticipated that oxidative stress in the wound should show a decreasing trend over the period of wound healing (Figure 10). This trend could be easily attributed to the radical-scavenging (antioxidant) activity of curcumin, resulting in lower SOD levels in cells at the wound site, as indeed was apparent (Figure 10). This indicated an improvement in the wound-healing environment and also supported the notion of a controlled release of curcumin from the micelle-hydrogel composite, slowly over a period of time, keeping the oxidative stress in check. High SOD activity in the control and blank groups confirmed these conclusions (Figure 10).

Upon scavenging, superoxide radicals in the tissue are converted to hydrogen peroxide. Hydrogen peroxide is toxic to cells and hampers the wound healing process, by causing oxidative stress, albeit one that is milder than the oxidative stress associated with superoxide radicals.[65, 66] This, in turn, stimulates the expression of the peroxide-scavenging enzyme catalase. Indeed, catalase activity generally increased in the wounded tissue, maintaining a low oxidative stress in the surrounding therein (Figure 11). Consequently, in the LC and HC groups, SOD activity was low, and catalase activity was high. Even though SOD activity was significantly lower in the HC group than that in the blank or control groups (Figure 10), catalase activity in the HC group was slightly higher than that in the LC group, and significantly higher than that in the blank and control

groups. Considering the low SOD activity and high catalase activity in the granulation tissues in the HC group, wound-healing efficacy was the highest in that group among all groups examined.

Combination of various histopathological analysis of wounds in the HC, LC, blank, and control groups on days 4 and 8 after surgery revealed that they indeed were in different stages of wound healing. As discussed earlier, the proliferative and maturation phases mark improved wound healing, with angiogenesis and connective tissue (collagen) deposition taking place in those phases. The presented results unambiguously supported the notion that the developed dual-drug–loaded micelle-hydrogel composites improved wound healing. Namely, in agreement with advanced granulation and re-epithelialization, and reduced inflammation, HC-treated wounds attained the late proliferative phase, with enhanced accumulation of collagen fibers in the extracellular matrix (Figure 12). Similarly, in the LC group, the total collagen content of the wound was higher than that in the blank and control groups, indicating improved wound healing. New collagen is observed in tissue as early as on the day of scarring. However, the newly formed collagen is not strong and as the wound matures, the amount and deposition of collagen changes, strengthening the tissue bed and increasing the tensile strength of the new formed tissue. Consequently, high level of collagen is an optimistic indicator of improved wound healing.

Since the pre-existing vascular network around the wound is not sufficient to provide ample nutrients and oxygen to the injury site, vessel damage at the wound site leads to ischemia.[67, 68] Therefore, the maintenance of cell viability in the wound and continuation of rapid healing essentially requires the formation of new vasculature, i.e., angiogenesis.[69] Angiogenesis involves the synthesis of new blood vessels from dividing differentiated endothelial cells of the local vascular system, mononuclear cells, and bone marrow-derived circulating endothelial cells.[70] While it remains debatable whether circulating cells escalate the formation of the luminal

endothelium layer, many studies demonstrated that circulating $CD31^+$ endothelial cells can indeed form new blood vessels.[71] Consequently, we investigated the presence of circulating $CD31^+$ cells at the wound site. The experiment revealed angiogenesis in the vicinity of the wounded area in the LC- and HC-treated groups, which confirmed the notion of improved wound healing in the treated groups (Figure 13). However, further studies are required to unequivocally verify this, since circulating macrophages also show CD31-positivity.[72] Collectively, the presented data were in agreement with the original hypothesis that the micelle-hydrogel composite would facilitate wound healing in case of trauma or skin patch excision.

Although the micelle-hydrogel composite performed well in the *in vivo* wound-healing model, amphotericin B was added only in trace amounts. Hence, an obvious question arises about whether loading the composite with one drug only would facilitate healing, and why two micelle types or two drugs in the composite were required. The composite system was used because the wounding was done in a controlled environment, which is not always the case out of the laboratory, and the second drug (at high concentration and defined dosage) is likely to be always required to accelerate healing. The drug can be a broad-spectrum antibiotic or a growth factor. In addition, the second micelle in the composite is required to maintain the structural integrity of the composite by electrostatic interactions between the micelles. As shown in Figure 14, the storage and loss moduli were substantially reduced in the absence of PGA-PPA micelles. That is because the two micelles types in the composite are oppositely charged, and during mixing and cross-linking they are involved in electrostatic interactions, stabilizing the system even in the absence of drug, and maintaining the integrity of the micelle-hydrogel composite. Furthermore, the hydrophobic core of the micelle in the composite acts as the drug reservoir. We hypothesized that the (hydrophobic) drug is involved in some kind of hydrophobic interactions with the core chains of the micelle.

Should that be so, the overall mechanical strength of the composite should change with drug release, as the core becomes looser with the diffusion of the drug. To evaluate this, we undertook a time-dependent rheological evaluation of the composite. Indeed, we observed a clear decreasing trend in the mechanical modulus of the composites at different time points of drug release (Figure 15). The gradual reduction in the modulus might indirectly reflect a slow and gradual drug release. That was important for the current study, as a sudden or burst-type release of curcumin can have several adverse effects. As shown in previous studies, a burst or high-dose release of curcumin at a wound site can cause DNA damage or chromosomal alterations (in rare cases), and delay wound healing.[73, 74] Further, the mechanical evaluation confirmed that the storage modulus of the devised micelle-hydrogel system was within the limits for gel systems used in wound healing and, hence, was an ideal candidate for such a gel.

In summary, the reported experiments and their implications indicate that the novel micelle-hydrogel composite can serve as effective would-healing material for enhanced skin repair and regeneration, aided by controlled release of encapsulated drugs. The composite positively impacted each stage of wound repair and healing, resulting in enhanced wound contraction, granulation, and re-epithelialization, and with a minimal inflammatory response. This suggests that the composite is extremely biocompatible and non-toxic for animal use. The exact mechanistic effect on wound healing remains unknown. However, even in the absence of encapsulated drug, no detrimental effects on the process of wound healing were observed (in the blank group in comparison with the control group). Consequently, this type of material could be optimized to enhance wound healing and developed as dressing material for clinical use.

Acknowledgments

The authors have no conflicts of interest to declare.

Monika Patel
School of Materials Science
Japan Advanced Institute of Science and Technology, 1-1, Asahidai, Nomi, Ishikawa, 923-1292, Japan

Tadashi Nakaji-Hirabayashi
Graduate School of Science and Engineering, University of Toyama, 3190, Gofuku, Toyama, Japan 930-8555
Graduate School of Innovative Life Science, University of Toyama, 3190 Gofuku, Toyama, Japan 930-8555

Kazuaki Matsumura
E-mail: mkazuaki@jaist.ac.jp
School of Materials Science
Japan Advanced Institute of Science and Technology, 1-1, Asahidai, Nomi, Ishikawa, 923-1292, Japan

References

1. Gelinsky E. Regarding wound healing and dressing material problems once from a different point. Bruns' Beitrage zur klinischen Chirurgie.1957;194:51-73.

2. Patrulea V, Ostafe V, Borchard G, Jordan O. Chitosan as a starting material for wound healing applications. European journal of pharmaceutics and biopharmaceutics : official journal of Arbeitsgemeinschaft fur Pharmazeutische Verfahrenstechnik eV. 2015;97:417-26.

3. Wharram SE, Zhang X, Kaplan DL, McCarthy SP. Electrospun silk material systems for wound healing. Macromol. Biosci. 2010;10:246-57.

4. Saraceno R, Chiricozzi A, Nistico SP, Tiberti S, Chimenti S. An occlusive dressing containing betamethasone valerate 0.1% for the treatment of prurigo nodularis. J Dermatolog Treat. 2010;21:363-6.

5. Yamamoto N, Kiyosawa T. Histological effects of occlusive dressing on healing of incisional skin wounds. Int Wound J. 2014;11:616-21.

6. Zadeh Farahani RM, Shahidi A. Occlusive dressing of wounds: old tradition, new concepts. J Tissue Viability. 2009;18:57-8.

7. Khan MI, Islam JM, Kabir W, Rahman A, Mizan M, Rahman MF, et al. Development of hydrocolloid Bi-layer dressing with bio-adhesive and non-adhesive properties. Mater. Sci. Eng. C. 2016;69:609-15.

8. Yanagibayashi S, Kishimoto S, Ishihara M, Murakami K, Aoki H, Takikawa M, et al. Novel hydrocolloid-sheet as wound dressing to stimulate healing-impaired wound healing in diabetic db/db mice. Biomed Mater Eng. 2012;22:301-10.

513 9. Rakhshaei R, Namazi H. A potential bioactive wound dressing based on carboxymethyl
514 cellulose/ZnO impregnated MCM-41 nanocomposite hydrogel. Mater. Sci. Eng. C. 2017;73:456-
515 64.
516 10. Rezvanian M, Ahmad N, Mohd Amin MC, Ng SF. Optimization, characterization, and in vitro
517 assessment of alginate-pectin ionic cross-linked hydrogel film for wound dressing applications.
518 Int J Biol Macromol 2017;97:131-40.
519 11. Wathoni N, Motoyama K, Higashi T, Okajima M, Kaneko T, Arima H. Physically crosslinked-
520 sacran hydrogel films for wound dressing application. Int J Biol Macromol 2016;89:465-70.
521 12. Brooks MP. Wound healing: a review. : J Miss State Med Assoc. 1973;14:385-90.
522 13. Kirker KR, James GA. In vitro studies evaluating the effects of biofilms on wound-healing
523 cells: a review. APMIS. 2017;125:344-52.
524 14. Atiyeh BS, Costagliola M, Hayek SN, Dibo SA. Effect of silver on burn wound infection
525 control and healing: review of the literature. Burns. 2007;33:139-48.
526 15. Babavalian H, Latifi AM, Shokrgozar MA, Bonakdar S, Mohammadi S, Moosazadeh
527 Moghaddam M. Analysis of Healing Effect of Alginate Sulfate Hydrogel Dressing Containing
528 Antimicrobial Peptide on Wound Infection Caused by Methicillin-Resistant Staphylococcus
529 aureus. Jundishapur J.Microbiol. 2015;8:e28320.
530 16. Betts J. Review: wound cleansing with water does not differ from no cleansing or cleansing
531 with other solutions for rates of wound infection or healing. Evid Based Nurs. 2003;6:81
532 17. Jagetia GC, Rajanikant GK. Acceleration of wound repair by curcumin in the excision wound
533 of mice exposed to different doses of fractionated gamma radiation. Int Wound J 2012;9:76-92.

534 18. Laplante AF, Germain L, Auger FA, Moulin V. Mechanisms of wound reepithelialization:
535 hints from a tissue-engineered reconstructed skin to long-standing questions. FASEB.
536 2001;15:2377-89.
537 19. Hunt DL. Review: debridement using hydrogel seems to be better than standard wound care
538 for healing diabetic foot ulcer. ACP J Club. 2003;139:16
539 20. Boury-Jamot M, Daraspe J, Bonte F, Perrier E, Schnebert S, Dumas M, et al. Skin aquaporins:
540 function in hydration, wound healing, and skin epidermis homeostasis. Handbook Exp Pharmacol.
541 2009:205-17.
542 21. Posthauer ME. Hydration: does it play a role in wound healing? Adv Skin Wound Care.
543 2006;19:74-6.
544 22. Rippon MG, Ousey K, Cutting KF. Wound healing and hyper-hydration: a counterintuitive
545 model. J Wound Care. 2016;25:68, 70-5.
546 23. Ishihara M, Ono K, Sato M, Nakanishi K, Saito Y, Yura H, et al. Acceleration of wound
547 contraction and healing with a photocrosslinkable chitosan hydrogel. Wound Repair Regen.
548 2001;9:513-21.
549 24. Luo Y, Diao H, Xia S, Dong L, Chen J, Zhang J. A physiologically active polysaccharide
550 hydrogel promotes wound healing. J Biomed Mater Res A. 2010;94:193-204.
551 25. Singh U, Barik A, Singh BG, Priyadarsini KI. Reactions of reactive oxygen species (ROS)
552 with curcumin analogues: Structure-activity relationship. Free Radic Res. 2011;45:317-25.
553 26. Zheng XH, Shao YX, Li Z, Liu M, Bu X, Luo HB, et al. Quantitative structure-retention
554 relationship of curcumin and its analogues. J Sep Sci. 2012;35:505-12.

555 27. Roy M, Sinha D, Mukherjee S, Biswas J. Curcumin prevents DNA damage and enhances the
556 repair potential in a chronically arsenic-exposed human population in West Bengal, India. Eur J
557 Cancer Prev. 2011;20:123-31.
558 28. Hashem MM, Atta AH, Arbid MS, Nada SA, Asaad GF. Immunological studies on Amaranth,
559 Sunset Yellow and Curcumin as food colouring agents in albino rats. Food Chem Toxicol.
560 2010;48:1581-6.
561 29. Ukil A, Maity S, Karmakar S, Datta N, Vedasiromoni JR, Das PK. Curcumin, the major
562 component of food flavour turmeric, reduces mucosal injury in trinitrobenzene sulphonic acid-
563 induced colitis. Br J Pharmacol. 2003;139:209-18.
564 30. Choudhury AK, Raja S, Mahapatra S, Nagabhushanam K, Majeed M. Synthesis and Evaluation
565 of the Anti-Oxidant Capacity of Curcumin Glucuronides, the Major Curcumin Metabolites.
566 Antioxidants. 2015;4:750-67.
567 31. Weber WM, Hunsaker LA, Abcouwer SF, Deck LM, Vander Jagt DL. Anti-oxidant activities
568 of curcumin and related enones. Bioorg Med Chem. 2005;13:3811-20.
569 32. Menon VP, Sudheer AR. Antioxidant and anti-inflammatory properties of curcumin. Adv Exp
570 Med Bio. 2007;595:105-25.
571 33. Wessler S, Muenzner P, Meyer TF, Naumann M. The anti-inflammatory compound curcumin
572 inhibits Neisseria gonorrhoeae-induced NF-kappaB signaling, release of pro-inflammatory
573 cytokines/chemokines and attenuates adhesion in late infection. J Biol Chem. 2005;386:481-90.
574 34. Xie M, Fan D, Zhao Z, Li Z, Li G, Chen Y, et al. Nano-curcumin prepared via supercritical:
575 Improved anti-bacterial, anti-oxidant and anti-cancer efficacy. Int. J. Pharm. 2015;496:732-40.

576 35. Umar S, Shah MA, Munir MT, Yaqoob M, Fiaz M, Anjum S, et al. Synergistic effects of
577 thymoquinone and curcumin on immune response and anti-viral activity against avian influenza
578 virus (H9N2) in turkeys. Poult Sci. 2016;95:1513-20.
579 36. Zhang W, Cui T, Liu L, Wu Q, Sun L, Li L, et al. Improving Anti-Tumor Activity of Curcumin
580 by Polymeric Micelles in Thermosensitive Hydrogel System in Colorectal Peritoneal
581 Carcinomatosis Model. J Biomed Nanotechnol. 2015;11:1173-82.
582 37. Patel M, Kaneko T, Matsumura K. Switchable release nano-reservoirs for co-delivery of drugs
583 via a facile micelle-hydrogel composite. J Mater Chem B. 2017;5:3488-97.
584 38. Freeman R, King B. Technique for the performance of the nitro-blue tetrazolium (NBT) test.
585 J Clin Pathol. 1972;25:912-4.
586 39. Hugo A. Catalase In vitro. Methods Enzymol. 1984;105C:121-6.
587 40. Nagoba BS, Suryawanshi NM, Wadher B, Selkar S. Acidic Environment and Wound Healing:
588 A Review. Wounds. 2015;27:5-11.
589 41. Mori HM, Kawanami H, Kawahata H, Aoki M. Wound healing potential of lavender oil by
590 acceleration of granulation and wound contraction through induction of TGF-beta in a rat model.
591 BMC Complement Altern Med. 2016;16:144.
592 42. Moulin V, Auger FA, Garrel D, Germain L. Role of wound healing myofibroblasts on re-
593 epithelialization of human skin. Burns. 2000;26:3-12.
594 43. Raja, Sivamani K, Garcia MS, Isseroff RR. Wound re-epithelialization: modulating
595 keratinocyte migration in wound healing. Front Biosci. 2007;12:2849-68.
596 44. King DF, King LA. A brief historical note on staining by hematoxylin and eosin. The Am J
597 Dermatopathol. 1986;8:168.

598 45. Oschman JL, Chevalier G, Brown R. The effects of grounding (earthing) on inflammation, the
599 immune response, wound healing, and prevention and treatment of chronic inflammatory and
600 autoimmune diseases. J Inflamm Res. 2015;8:83-96.
601 46. Resan M, Vukosavljevic M, Vojvodic D, Pajic-Eggspuehler B, Pajic B. The acute phase of
602 inflammatory response involved in the wound-healing process after excimer laser treatment. Clin
603 Ophthalmol. 2016;10:993-1000.
604 47. Wang Y, Fu X, Ma N. Relationship between wound healing and TNF, MDA and SOD contents
605 in granulation tissues of rats in the first week. Chinese journal of plastic surgery and burns.
606 1996;12:45-7.
607 48. Douglas DM, Forester JC, Ogilvie RR. Physical characteristics of collagen in the later stages
608 of wound healing. Br J Surg. 1969;56:219-22.
609 49. Grabska-Liberek I, Galus R, Owczarek W, Wlodarsk K, Zabielski S, Malejczyk J, et al.
610 Collagen based dressings in the treatment of wound healing. Pol Merkur Lekarsk. 2013;35:51-4.
611 50. Kamma-Lorger CS, Boote C, Hayes S, Albon J, Boulton ME, Meek KM. Collagen
612 ultrastructural changes during stromal wound healing in organ cultured bovine corneas. Exp Eye
613 Res. 2009;88:953-9.
614 51. Mussini E, Hutton JJ, Jr., Udenfriend S. Collagen proline hydroxylase in wound healing,
615 granuloma formation, scurvy, and growth. Science. 1967;157:927-9.
616 52. Van Waes, C. Cell adhesion and regulatory molecules involved in tumor formation, hemostasis,
617 and wound healing. Head Neck. 1995;17:140-147.
618 53. Koh T, DiPietro L. Inflammation and wound healing: The role of the macrophage. Expert Rev
619 Mol Med. 2011;13:E23.
620 54. Wilson HJ. Inflammation and wound healing. J Artif Organs. 2005;7:71-76.

621 55. Chikuma HM, Verkman, AS. Aquaporin-3 facilitates epidermal cell migration and
622 proliferation during wound healing. Int J Mol Med. 2008;86:221.
623 56. Reinders Y, Felthaus O, Brockhoff G, Pohl F, et al. Impact of Platelet-Rich Plasma on Viability
624 and Proliferation in Wound Healing Processes after External Radiation. Int J Mol Sci.
625 2017;18:1819.
626 57. Meir M, Flemming S, Burkard N, Bergauer L, Metzger M, et al. Glial cell line-derived
627 neurotrophic factor promotes barrier maturation and wound healing in intestinal epithelial cells in
628 vitro. Am J Physiol Gastrointest Liver Physiol. 2015;309(8): G613-24.
629 58. Ud‐Din S, Bayat A. Non‐invasive objective devices for monitoring the inflammatory,
630 proliferative and remodelling phases of cutaneous wound healing and skin scarring. Exp Dermatol.
631 2016;25:579-585.
632 59. Okizaki S, Ito Y, Hosono K, Oba K, Ohkubo H, Kojo K, et al. Vascular Endothelial Growth
633 Factor Receptor Type 1 Signaling Prevents Delayed Wound Healing in Diabetes by Attenuating
634 the Production of IL-1beta by Recruited Macrophages. Am J Pathol. 2016;186:1481-98.
635 60. Jia S, Xie P, Hong S J, Galiano R, Singer A, Clark R, Mustoe T. Intravenous curcumin efficacy
636 on healing and scar formation in rabbit ear wounds under non-ischemic, ischemic, and ischemia-
637 reperfusion conditions. Wound Repair Regen. 2014;22.
638 61. E. E. Peacock Jr . Wound repair. Third edition. 1984. 526p.
639 62. Martin P. Wound Healing--Aiming for Perfect Skin Regeneration. Science. 1997;276:75-81.
640 63. Hunt T, Dunphy JE. Fundamentals of wound management. New York: Appleton-
641 CenturyCrofts, 1979.
642 64. Carrasco L, María I C, Blázquez-Castro A, Vecchio D, et al. Photoactivation of ROS
643 Production In Situ Transiently Activates Cell Proliferation in Mouse Skin and in the Hair Follicle

644 Stem Cell Niche Promoting Hair Growth and Wound Healing. J Invest Dermatol.
645 2015;135(11):2611-22.
646 65. Gong C Y, Wu Q, Wang Y J, Zhang D D, Luo F, et al. A biodegradable hydrogel system
647 containing curcumin encapsulated in micelles for cutaneous wound healing. Biomaterials.
648 2013;34:6377-87.
649 66. Bae G U, Seo D W, Kwon H K, Lee H Y, Hong S, et al. Hydrogen Peroxide Activates p70S6k
650 Signaling Pathway. World J Biol Chem. 1999;274:32596.
651 67. Arnold F, West DC. Angiogenesis in wound healing. Pharmacol Therapeut. 1991;52:407-22.
652 68. Yoshida S, Yoshimoto H, Hirano A, Akita S. Wound Healing and Angiogenesis through
653 Combined Use of a Vascularized Tissue Flap and Adipose-Derived Stem Cells in a Rat Hindlimb
654 Irradiated Ischemia Model. Plast Reconstr Surg. 2016;137:1486-97.
655 60. Grunewald M, Avraham I, Dor Y, Bachar-Lustig E, Itin A, Jung S, et al. VEGF-induced adult
656 neovascularization: recruitment, retention, and role of accessory cells. Cell. 2006;124:175-89.
657 70. Urbich C, Dimmeler S. Endothelial progenitor cells: characterization and role in vascular
658 biology. Circ Res. 2004;95:343-53.
659 71. Galiano R D, Tepper O M, Pelo C R, Bhatt K A, Callaghan M, et al.Topical Vascular
660 Endothelial Growth Factor Accelerates Diabetic Wound Healing through Increased Angiogenesis
661 and by Mobilizing and Recruiting Bone Marrow-Derived Cells. Am J Pathol. 2004;164(6):1935-
662 47.
663 72. Croix B S, Rago C, Velculescu V, Traverso1 G, Romans K E, et al. Genes Expressed in Human
664 Tumor Endothelium. Science. 2000;289:1197-1202.

73. Shang HS, Chang CH, Chou YR, Yeh MY, Au MK, Lu HF, et al. Curcumin causes DNA damage and affects associated protein expression in HeLa human cervical cancer cells. Oncol Rep. 2016;36:2207-15.

74. Lu HF, Yang JS, Lai KC, Hsu SC, Hsueh SC, Chen YL, et al. Curcumin-induced DNA damage and inhibited DNA repair genes expressions in mouse-rat hybrid retina ganglion cells. Neurochem Res. 2009;34:1491-7.

673 **Figure legends**

674 **FIGURE 1.** Schematic Representation of the Formulation of Micelle-Hydrogel Composite for
675 Drug Release. Amp B, amphotericin B; DMSO, dimethyl sulfoxide.

676 **FIGURE 2.** Schematic Representation and Actual Images of Wound Generation.

677 **FIGURE 3.** *In Vitro* Drug Release of Curcumin and Amphotericin B at Inflammatory pH (ca. 4.5).
678 Data Are Presented as Mean ± SD (n = 3).

679 **FIGURE 4.** Macroscopic Appearance of Wounds in Rats from Different Experimental Groups on
680 Days 0, 4, and 8. The Images Are Representative of Three Biological Replicates.

681 **FIGURE 5.** (a) Wound Closure (%) in Rats in Different Groups on Days 4 and 8, and (b) Residual
682 Wound Size in Treated Rats in Comparison with Day 0. $^{**}p < 0.05$. Data Are Presented as Mean
683 ± SD (n = 3).

684 **FIGURE 6.** The Thickness of Granulation Area in the Tested Animals. (a) Histological Evaluation
685 of the Newly Formed Granulated Tissue on day 8. The Images Are Representative of Three
686 Biological Replicates. (b) Comparison of the Granulation Thickness in Samples. $^{**}p < 0.05$. Data
687 Are Presented as Mean ± SD (n = 3).

688 **FIGURE 7.** Degree of Re-Epithelialization in Different Rat Groups on Days 4 and 8. $^{**}p < 0.05$
689 When Compared with the Control. Data Are Presented as Mean ± SD (n = 3).

690 **FIGURE 8.** Histological Evaluation of Epithelial Tissue Regeneration in Wounds in Different Rat
691 Groups. The Arrows Indicate the Wound Edge and the Dotted Lines Trace the Path of Re-
692 Epithelialization. The Images Are Representative of Three Biological Replicates.

693 **FIGURE 9.** Evaluation of Inflammatory Response by Hoechst 33258 and Iba1 Staining of Tissue
694 Sections from Different Rat Groups. Blue Dots Are the Nuclei of All Cells Stained by Hoechst

33258 and Green Dots Represent the Macrophage Cytosol Stained by Anti-Iba1 Antibodies. The Images Are Representative of Three Biological Replicates.

FIGURE 10. SOD Activity in the Wounded Tissue in Different Rat Groups on Days 4 and 8 After the Surgery. $^{**}p < 0.05$. Data Are Presented as Mean ± SD ($n = 3$).

FIGURE 11. Catalase Activity in the Wounded Tissue in Different Rat Groups on Days 4 and 8 After the Surgery. $^{**}p < 0.05$. Data Are Presented as Mean ± SD ($n = 3$).

FIGURE 12. The Amount of Collagen in Wounded Tissue in Different Rat Groups on Days 4 and 8 After the Surgery. $^{**}p < 0.05$. Data Are Presented as Mean ± SD ($n = 3$).

FIGURE 13. Evaluation of Angiogenesis in Different Rat Groups on 8 Day. Thin Sections Were Stained Using Anti-CD31 Antibodies. The Images Are Representative of Three Biological Replicates.

FIGURE 14. Storage (G′) and Loss (G″) Moduli of Micelle-Hydrogel Composites Containing PGA-PPA (a) and Gels without PGA-PPA (b), at 37°C. The Graphs Are Representative of 3 Replicates.

FIGURE 15. Storage (G′) and Loss (G″) Moduli of Micelle-Hydrogel Composites during Drug Release at 37°C. The Graphs Are Representative of 3 Replicates.

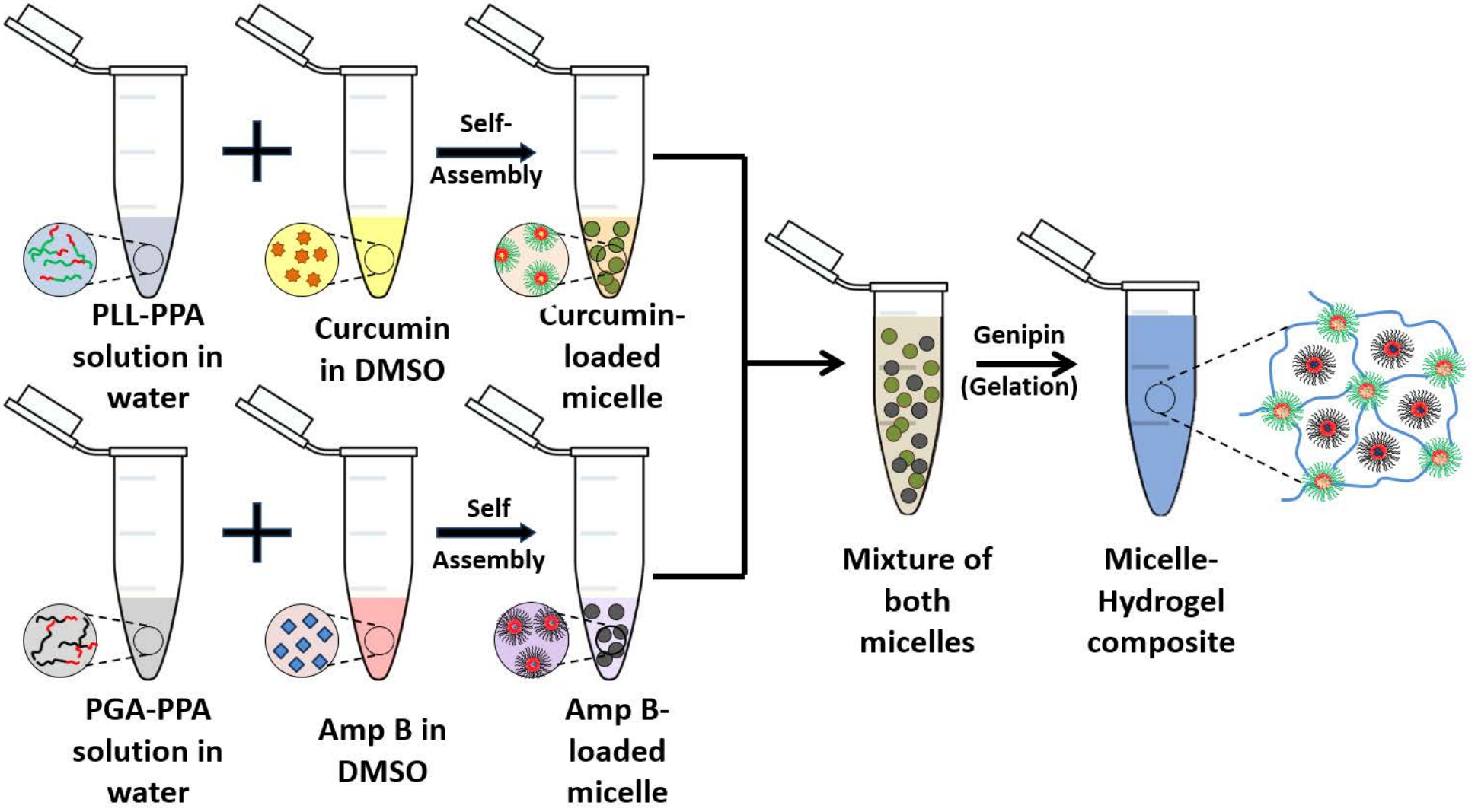
PLL-PPA solution in water
Curcumin in DMSO
Self-Assembly
Curcumin-loaded micelle
PGA-PPA solution in water
Amp B in DMSO
Self Assembly
Amp B-loaded micelle
Mixture of both micelles
Genipin (Gelation)
Micelle-Hydrogel composite

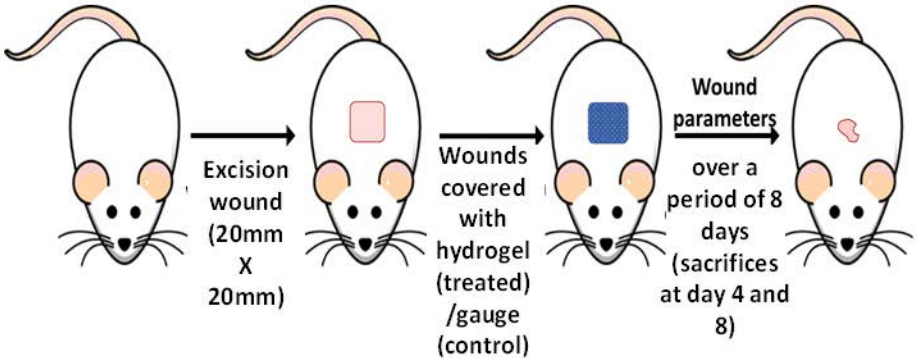
Excision wound (20mm X 20mm)
Wounds covered with hydrogel (treated) /gauge (control)
Wound parameters
over a period of 8 days (sacrifices at day 4 and 8)

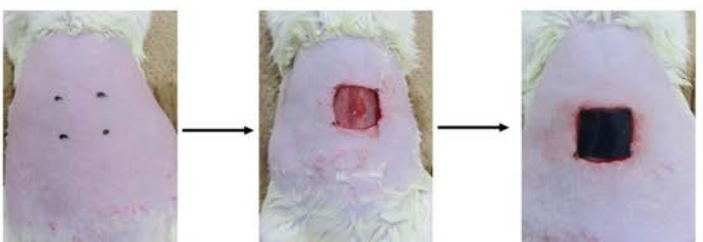
Template marking on rat
Creation of excision wound on dorsum
Hydrogel implant

Figure 3

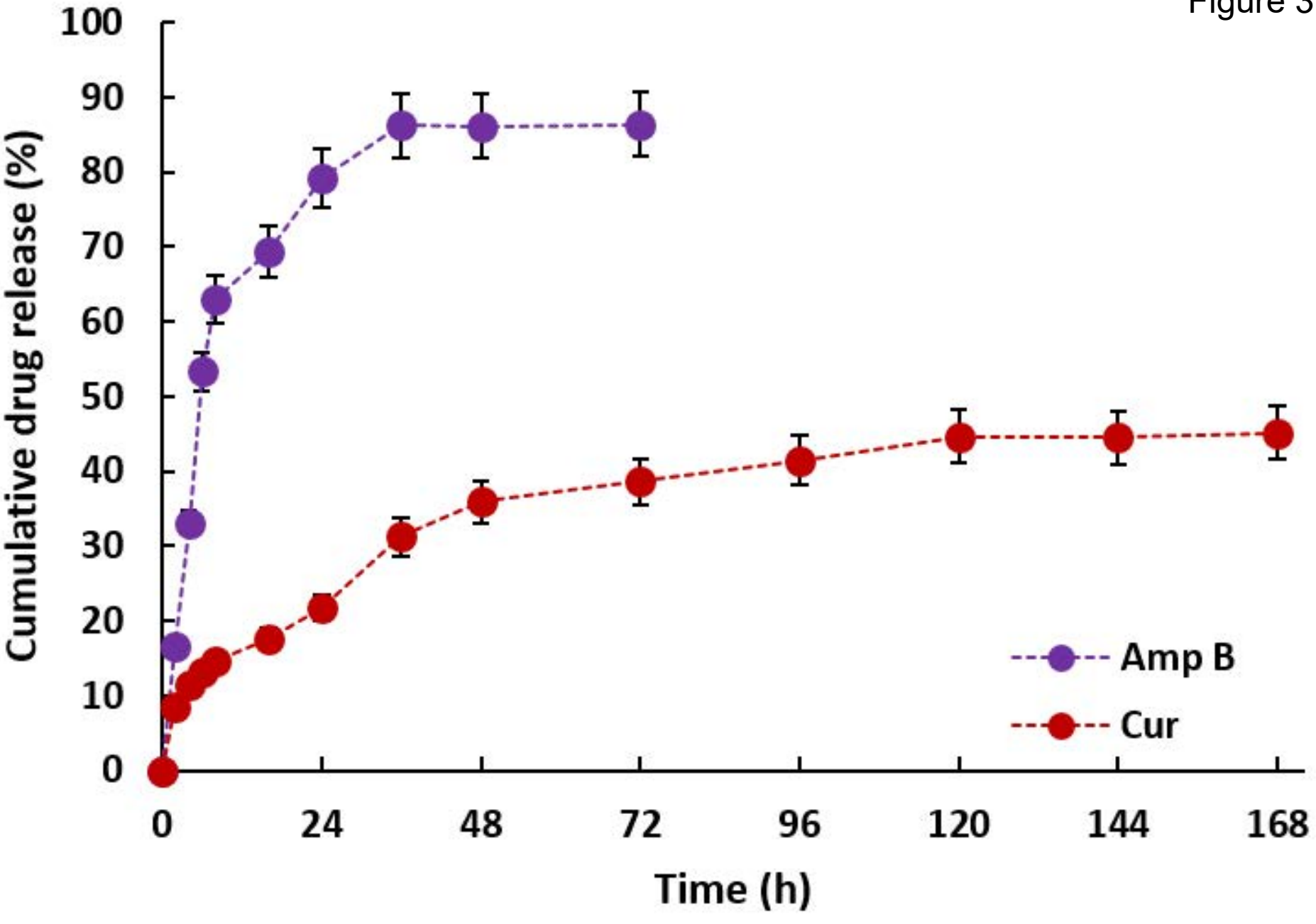
Cumulative drug release (%)
100
90
80
70
60
50
40
30
20
10
0
0
24
48
72
96
120
144
168
Time (h)
Amp B
Cur

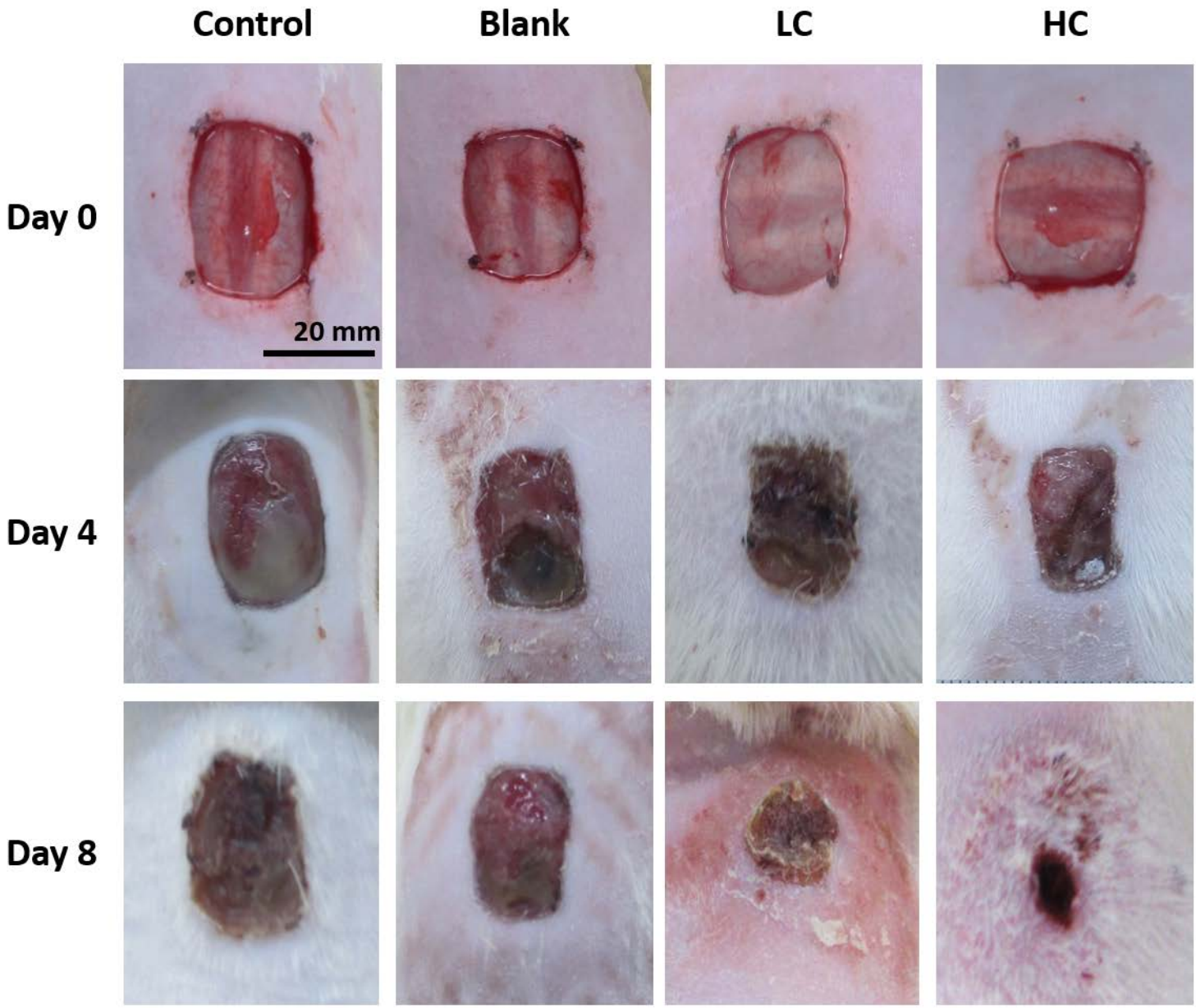
Control
Blank
LC
HC
Day 0
Day 4
Day 8
20 mm

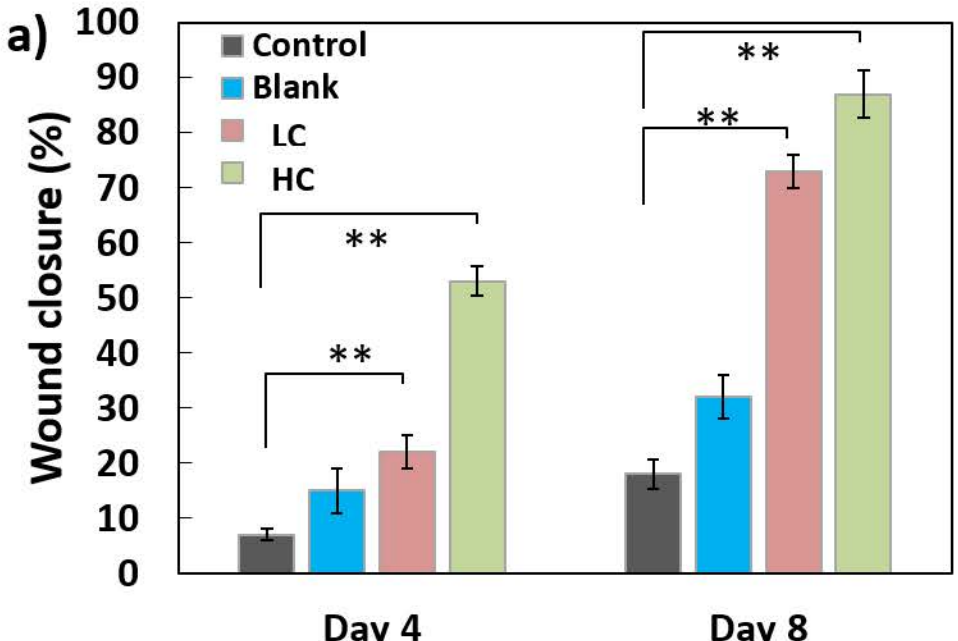
a)
Wound closure (%)
100
90
80
70
60
50
40
30
20
10
0
Control
Blank
LC
HC
**
**
**
**
Day 4
Day 8

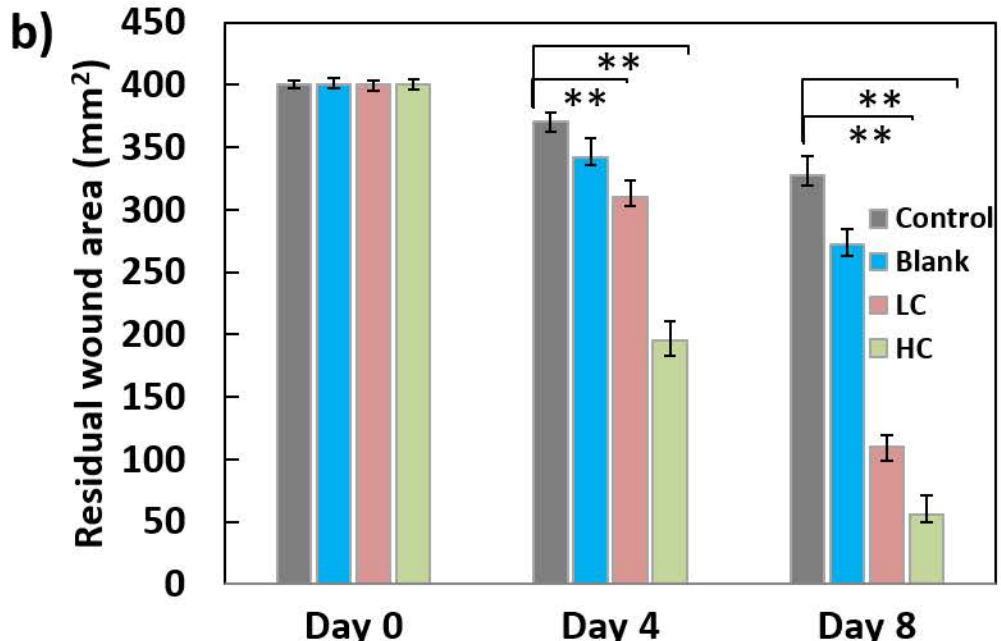
b)
Residual wound area (mm²)
450
400
350
300
250
200
150
100
50
0
**
**
**
**
Control
Blank
LC
HC
Day 0
Day 4
Day 8


a)
200.00000 μ m

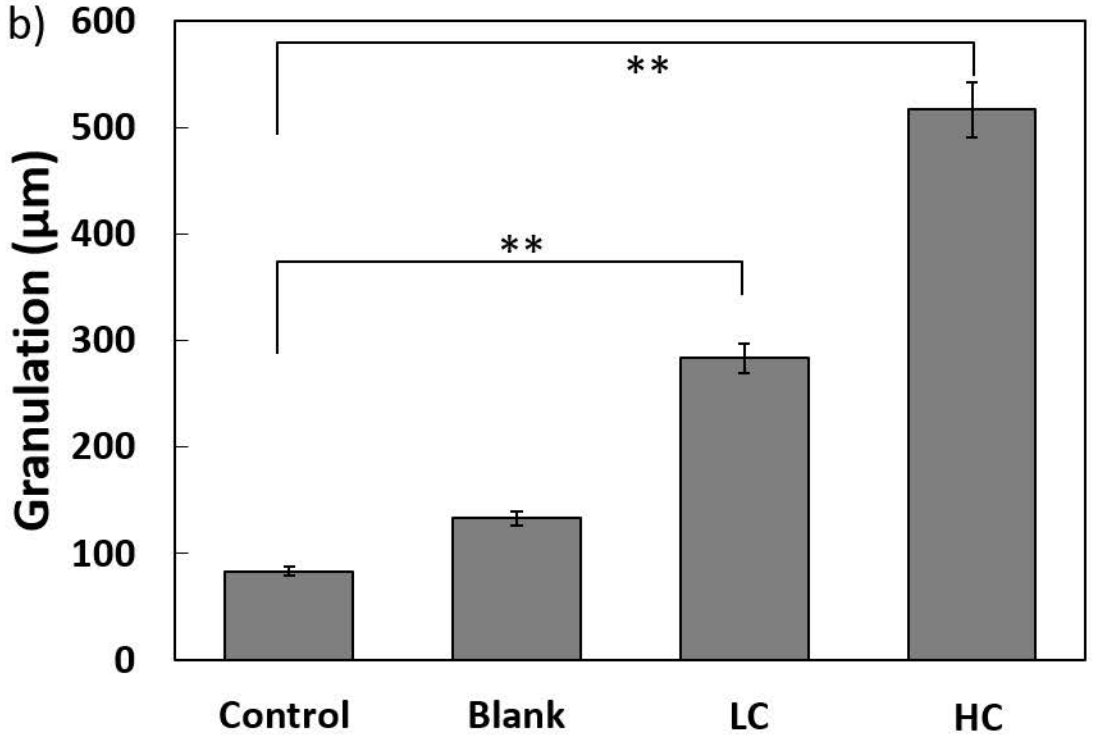
b)
Granulation (μm)
600
500
400
300
200
100
0
**
**
Control
Blank
LC
HC

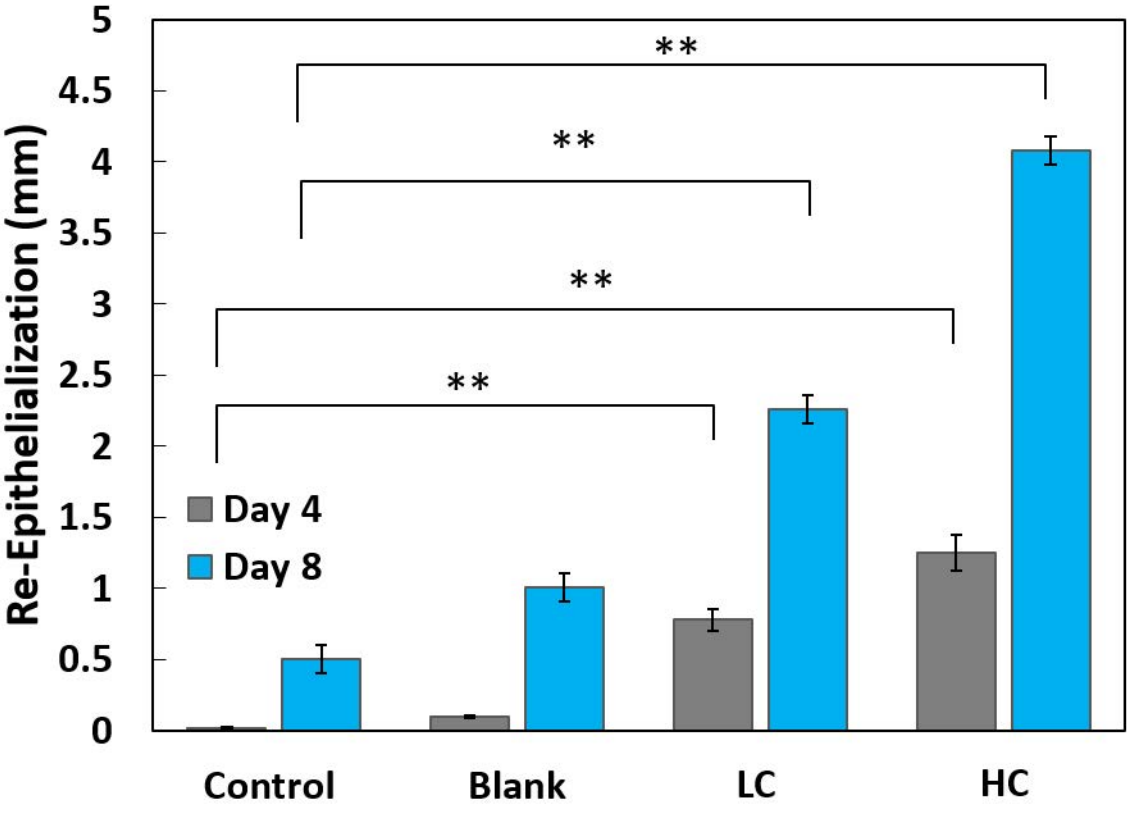
Re-Epithelialization (mm)
5
4.5
4
3.5
3
2.5
2
1.5
1
0.5
0
**
**
**
**
Day 4
Day 8
Control
Blank
LC
HC

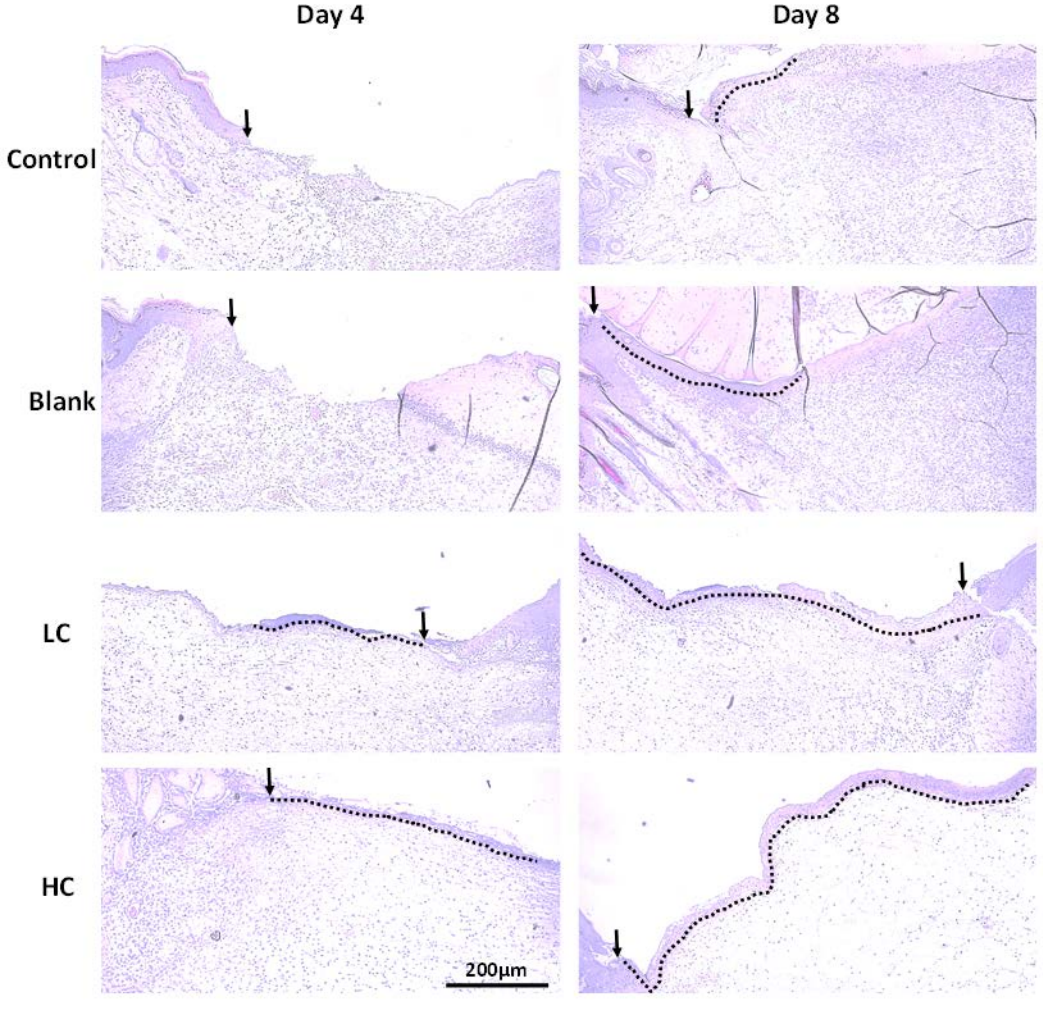
Day 4
Day 8
Control
Blank
LC
HC
200μm

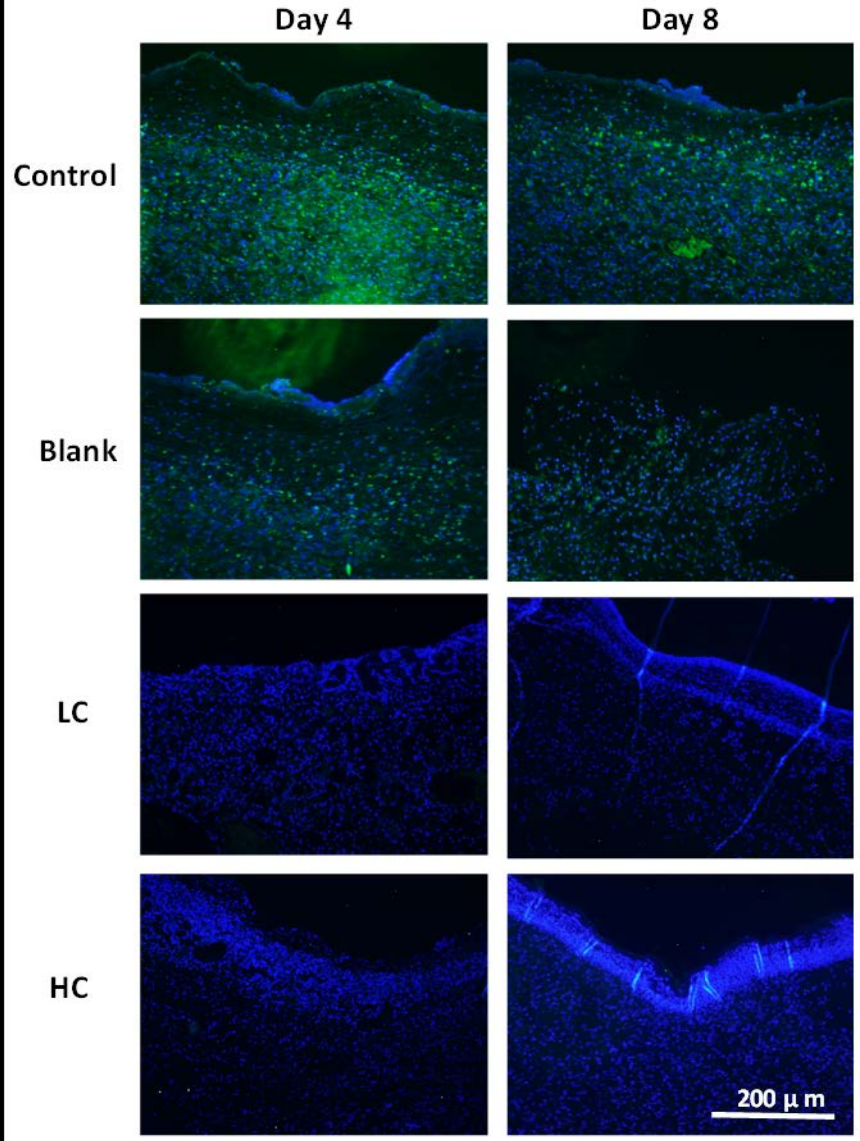
Day 4
Day 8
Control
Blank
LC
HC
200 µ m

Figure 10

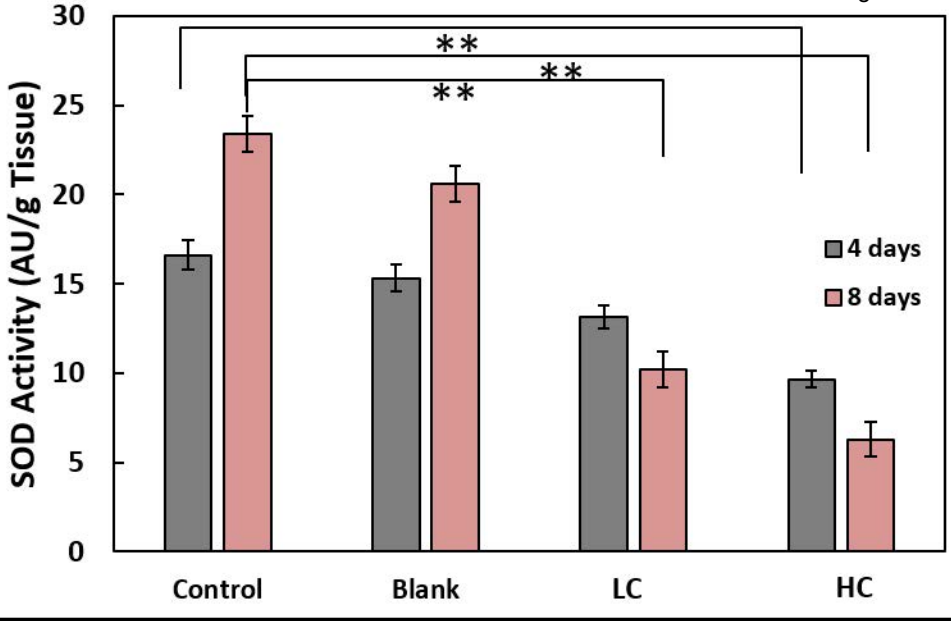
SOD Activity (AU/g Tissue)
30
25
20
15
10
5
0
**
**
**
4 days
8 days
Control
Blank
LC
HC

Figure 11

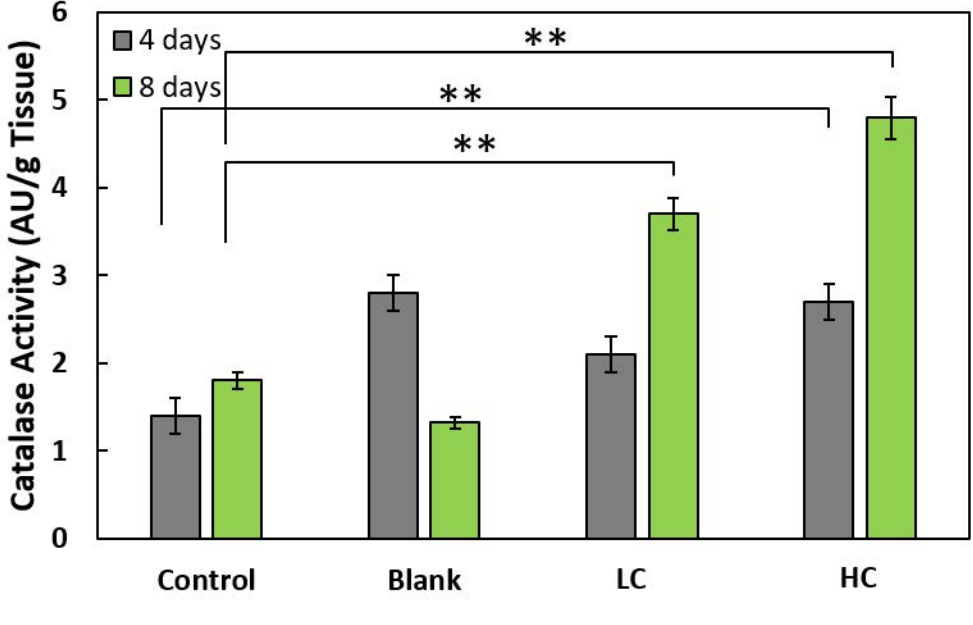
Catalase Activity (AU/g Tissue)
6
5
4
3
2
1
0
4 days
8 days
**
**
**
Control
Blank
LC
HC

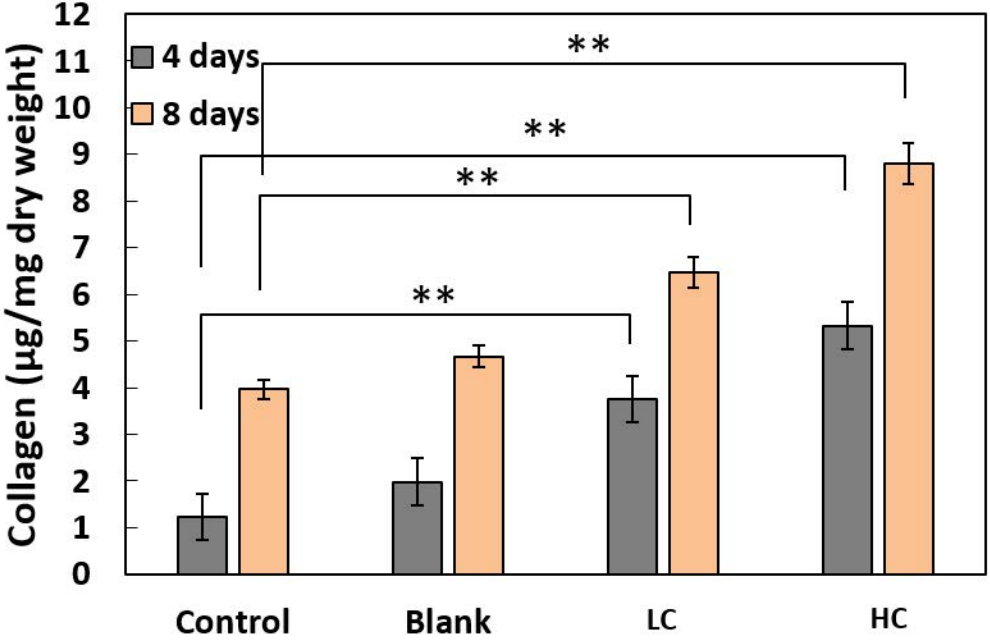
Collagen (μg/mg dry weight)
12
11
10
9
8
7
6
5
4
3
2
1
0
4 days
8 days
**
**
**
**
Control
Blank
LC
HC

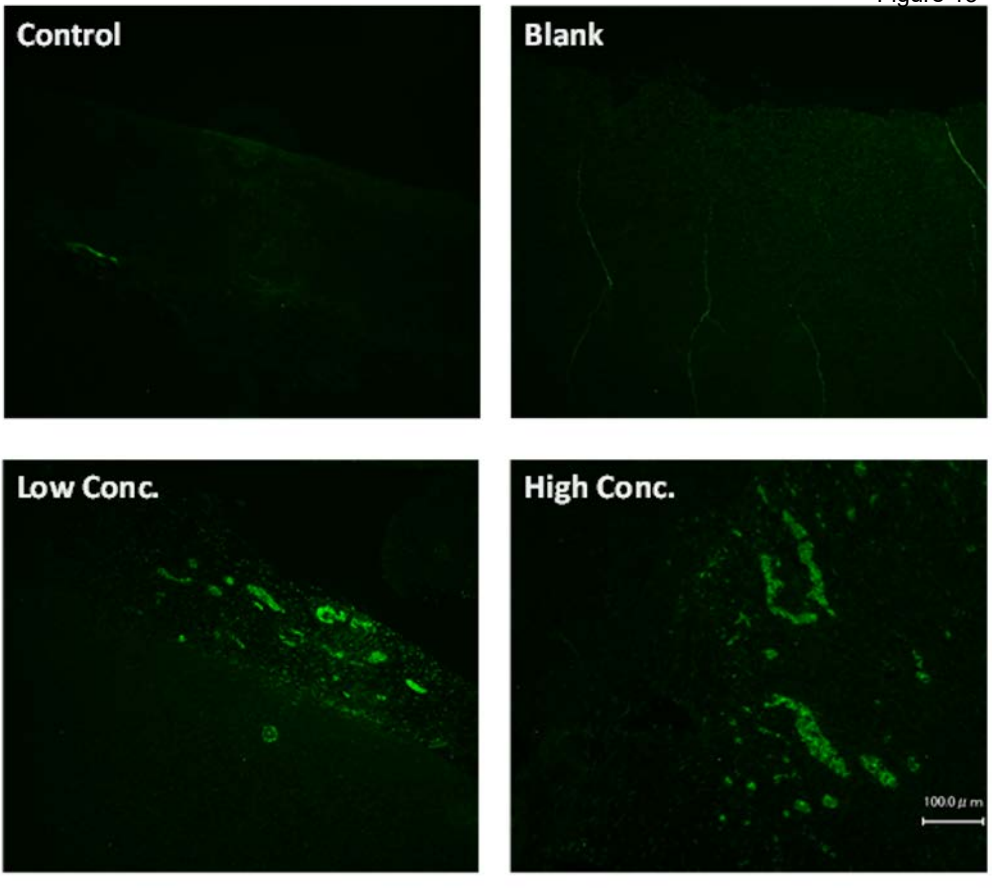
Control
Blank
Low Conc.
High Conc.
100.0 µm

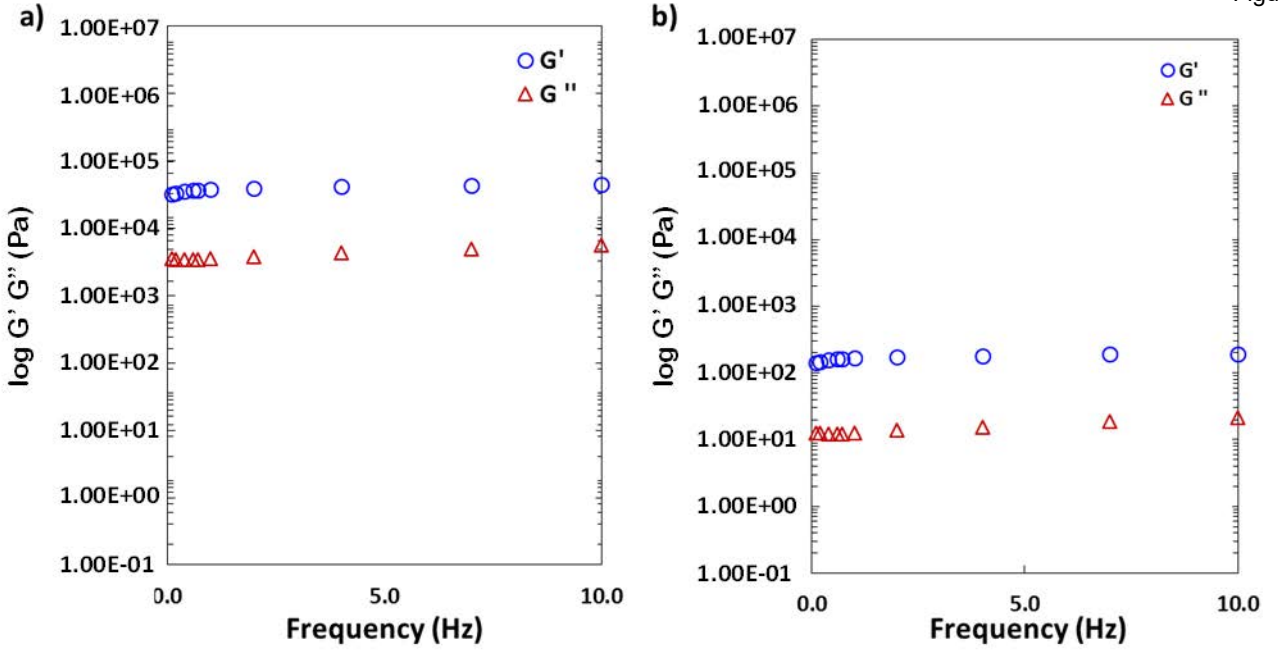
a)
1.00E+07
1.00E+06
1.00E+05
1.00E+04
1.00E+03
1.00E+02
1.00E+01
1.00E+00
1.00E-01
log G' G'' (Pa)
G'
G''
0.0
5.0
10.0
Frequency (Hz)
b)
1.00E+07
1.00E+06
1.00E+05
1.00E+04
1.00E+03
1.00E+02
1.00E+01
1.00E+00
1.00E-01
log G' G'' (Pa)
G'
G''
0.0
5.0
10.0
Frequency (Hz)

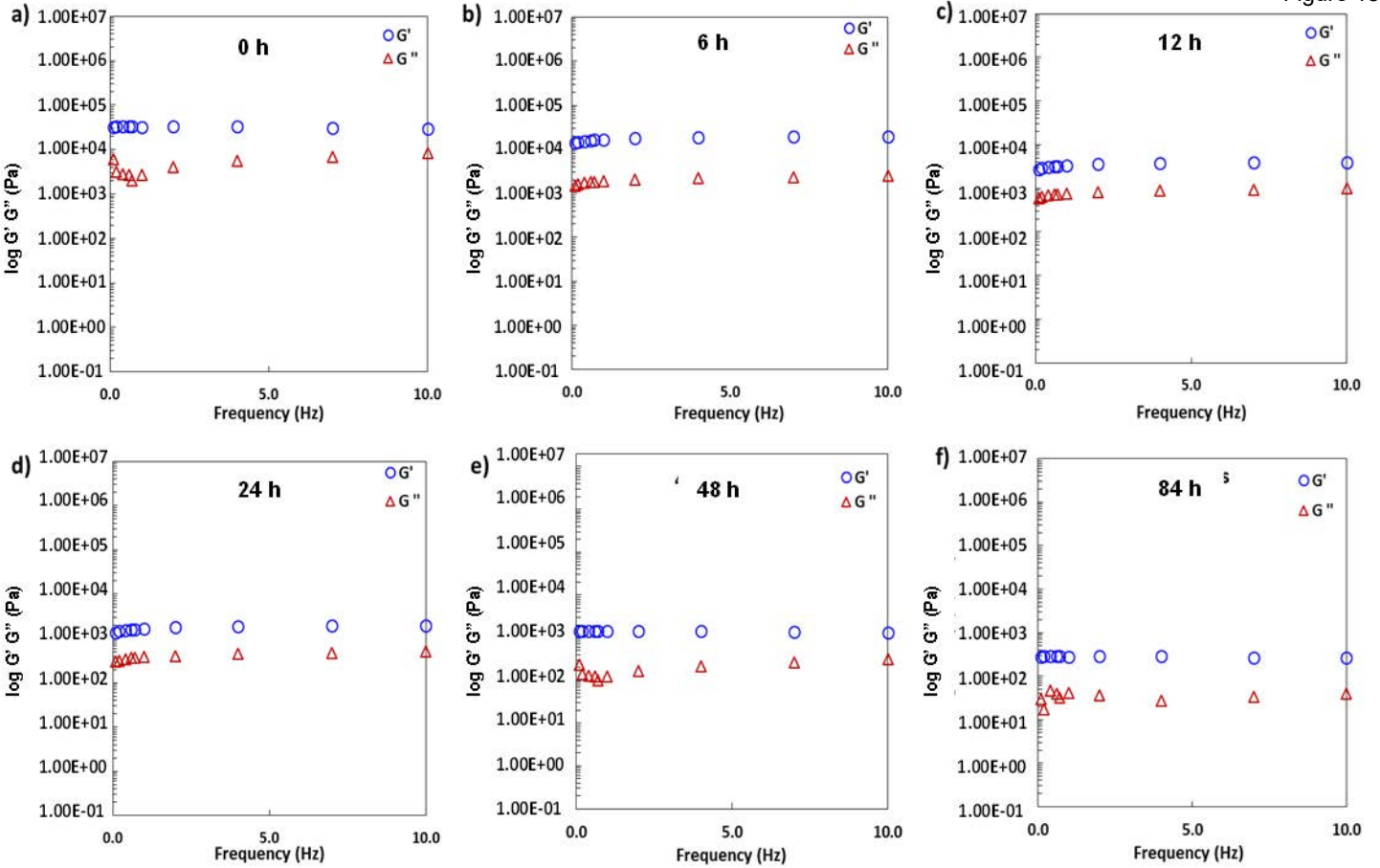
a)
0 h
b)
6 h
c)
12 h
d)
24 h
e)
48 h
f)
84 h
G'
G "
log G' G" (Pa)
Frequency (Hz)
1.00E+07
1.00E+06
1.00E+05
1.00E+04
1.00E+03
1.00E+02
1.00E+01
1.00E+00
1.00E-01
0.0
5.0
10.0

Effect of dual-drug–releasing micelle-hydrogel composite on wound healing *in vivo* in full-thickness excision wound rat model

Monika Patel[1], Tadashi Nakaji-Hirabayashi[2,3], Kazuaki Matsumura[1]*

[1] School of Materials Science, Japan Advanced Institute of Science and Technology, Ishikawa, 923-1292, Japan

[2] Graduate School of Science and Engineering ,University of Toyama, Toyama, 930-8555, Japan

[3]Graduate School of Innovative Life Science, University of Toyama, Toyama, 930-8555, Japan

SUPPORTING INFORMATION

Gel formation

Polymer synthesis. Two different di-block polypeptides were first prepared: poly(L-lysine)-*b*-poly(phenylalanine) (PLL-PPA) and poly(glutamic acid)-*b*-poly(phenylalanine) (PGA-PPA) (Scheme S1). The block copolymers PZLL-*b*-PPA and P(OBzl)GA-*b*-PPA were synthesized in a two-step reaction using the protected amino acid precursors ε-benzyloxycarbonyl-L-lysine [H-Lys(Z)-OH], γ-benzyl-L-glutamic acid [H-Glu(OBzl)-OH], and phenylalanine (H-Phe-OH). First, the hydrophilic block (of either glutamic acid or lysine) was synthesized by ring opening polymerization of the respective N-carboxyanhydride (NCA). Upon complete consumption of the first monomer, Phe-NCA was added as the second hydrophilic block, and the reaction carried out until complete consumption of the second block. The di-block polypeptides were precipitated in diethyl ether. These polypeptides were further protected in trifluoroacetic acid and HBr to yield PLL-PPA and PGA-PPA (Scheme S2).

Formation of drug-loaded micelles. To prepare drug-loaded micelles, 2% (w/v) solution of above synthesised amphiphilic polypeptides was prepared. This solution was then mixed with the desired amount of drug (dissolved in dimethyl sulfoxide) and dialyzed. After dialysis, the solution was lyophilized to yield drug-loaded micelles.

Preparation of hydrogel. To prepare, drug-loaded micelle-hydrogel composite, the two drug-loaded micelles (curcumin-loaded PLL-PPA and amphotericin B-loaded PGA-PPA) were mixed in 1:1 ratio. This mixture was cross-linked using a biocompatible cross-linker genipin, utilizing the free amino group in PLL-PPA polymers (Scheme S3).

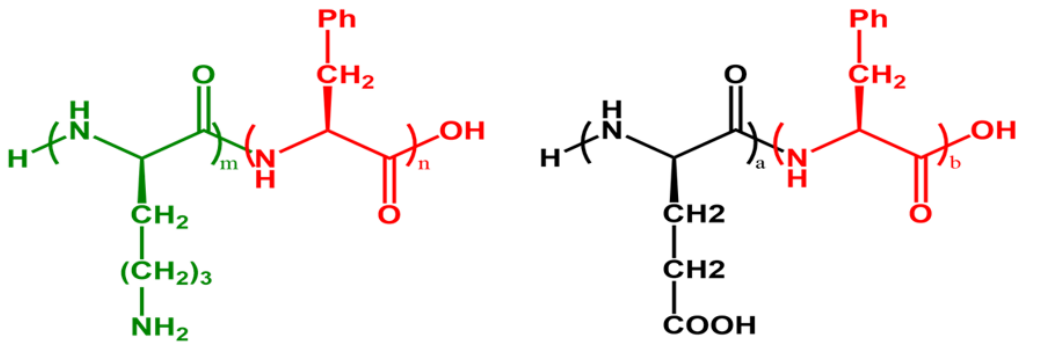

SCHEME S1. Schematic Diagrams of the Prepared Polymers.

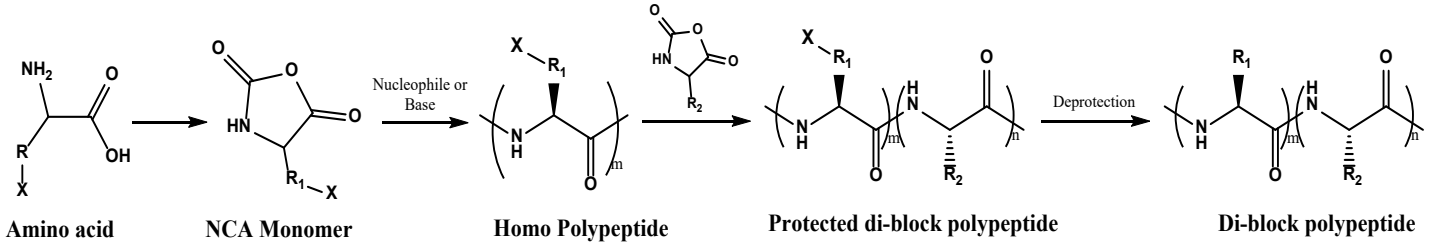

For amphiphillic polypeptide R_1 = -$(CH_2)_4$-NH_2 / -$(CH_2)_2$-COOH; R_2 = -CH_2-C_6H_5; X = Protection group

SCHEME S2. Schematic Representation of the NCA Polymerization Reaction.

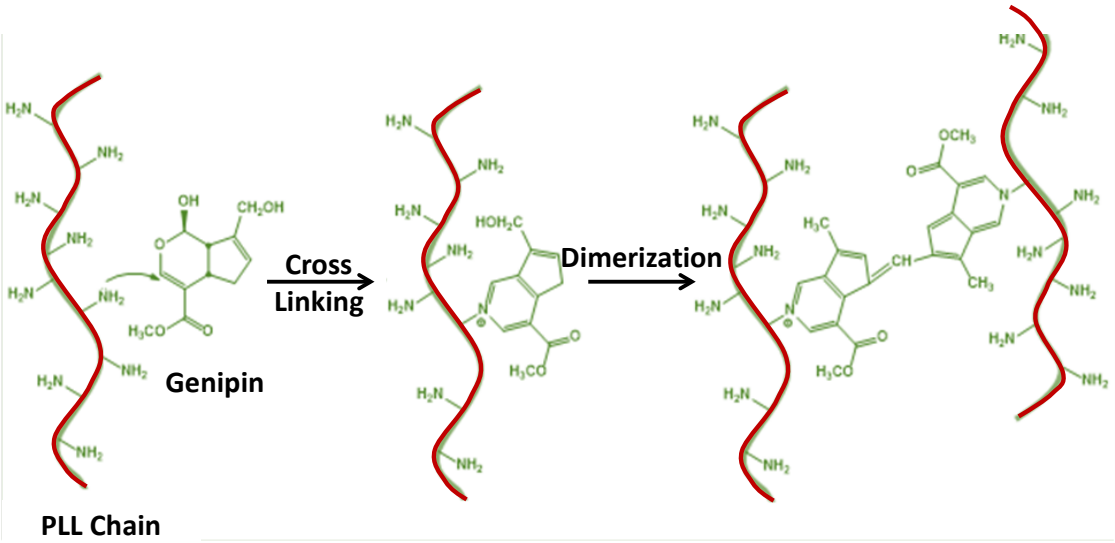

SCHEME S3. Schematic Representation of Genipin Crosslinking.

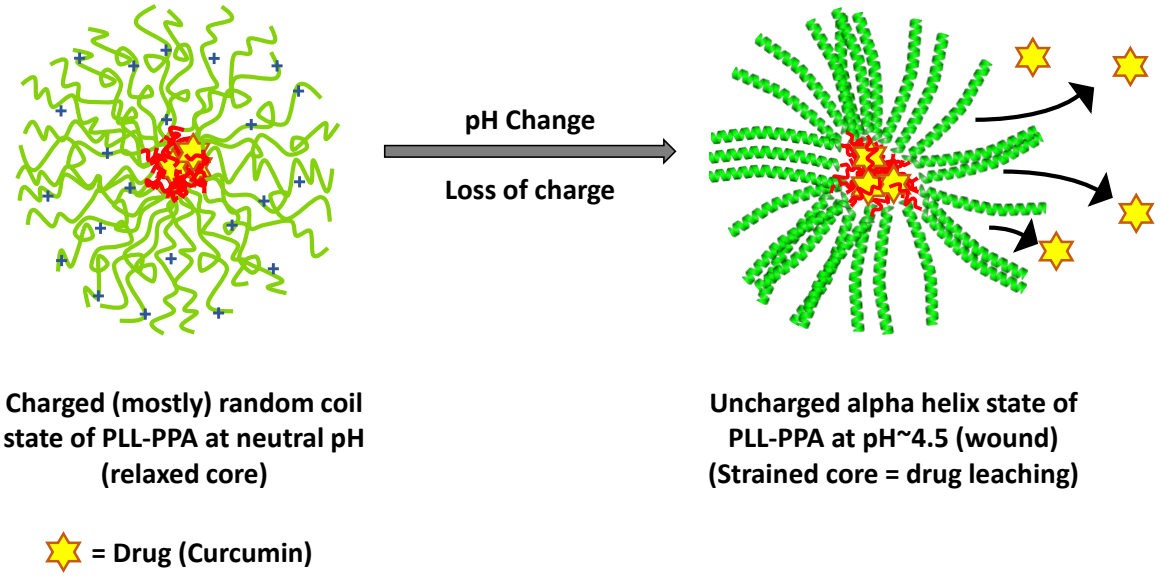

FIGURE S1. Schematic Representation of Effective Drug Release at Wound pH (ca. 4.5) from PLL-PPA Micelles in the Composite. Color Code: Green, PLL Block; Red, PPA Block.